Separation Science and Technology
Publication details, including instructions for authors and subscription information:
http://www.informaworld.com/smpp/title~content=t713708471

Some Modern Aspects of Ultracentrifugation

E. T. Adams Jr.[a]; Will E. Ferguson[a]; Peter J. Wan[a]; Jerry L. Sarquis[a]; Barnee M. Escott[a]
[a] CHEMISTRY DEPARTMENT, TEXAS A&M UNIVERSITY, COLLEGE STATION, TEXAS

To cite this Article Adams Jr., E. T. , Ferguson, Will E. , Wan, Peter J. , Sarquis, Jerry L. and Escott, Barnee M.(1975) 'Some Modern Aspects of Ultracentrifugation', Separation Science and Technology, 10: 2, 175 — 244
To link to this Article: DOI: 10.1080/00372367508059000
URL: http://dx.doi.org/10.1080/00372367508059000

SEPARATION SCIENCE, 10(2), pp. 175–244, 1975

SYMPOSIUM ON NEW METHODS OF SEPARATION (continued)

Some Modern Aspects of Ultracentrifugation

E. T. ADAMS, JR., WILL E. FERGUSON, PETER J. WAN, JERRY L. SARQUIS, and BARNEE M. ESCOTT

CHEMISTRY DEPARTMENT
TEXAS A&M UNIVERSITY
COLLEGE STATION, TEXAS 77843

Abstract

Shortly after the ultracentrifuge was developed, it was realized that molecular-weight distributions (MWDs) of polymers could be obtained from sedimentation equilibrium experiments. Although numerous attempts have been made to obtain MWDs from sedimentation equilibrium experiments, the results were not very satisfactory, and most MWDs were obtained from sedimentation velocity experiments. Only recently have some satisfactory methods been developed for sedimentation equilibrium experiments. These methods were restricted to ideal, dilute solutions and to ultracentrifuge cells with sector-shaped centerpieces. Both of these restrictions can now be removed. Methods for correcting for nonideal behavior are shown. Procedures for obtaining MWDs from sector—or nonsector—shaped centerpieces are shown. These procedures are illustrated with real examples, and a comparison between MWDs obtained by sedimentation velocity, sedimentation equilibrium, and gel permeation chromatography experiments is shown.

Self-associations can be studied by various thermodynamic methods (osmometry, light scattering, or sedimentation equilibrium) that give average or apparent average molecular weights as a function of associating solute concentration. Of the various thermodynamic methods, the sedimentation equilibrium experiment is the best way to study self-associations. Because of the interrelation between average or apparent average molecular weights, the theory developed originally for the sedimentation equilibrium experiment can be extended to other methods. We show methods for analyzing several types of self-associations, using real examples. The advantages of thermodynamic over transport methods for studying self-associations are discussed; furthermore, we show how thermodynamic and transport experiments can be combined to yield more information about the self-associating species.

INTRODUCTION

The year 1974 marks the fiftieth anniversary of the ultracentrifuge; the first paper using the term ultracentrifuge was published by Svedberg and Rinde in 1924 (*1*). In the ensuing years the ultracentrifuge has had a wide impact in various areas of chemistry, but its most influential role has been in biochemistry, where it has been described as one of the most important research instruments in the field (*2*). According to Svedberg (*1*, *3*), an ultracentrifuge has the following characteristics: it has a precise speed control; it has an optical system for viewing and/or photographing the experimental data; and it is free from convection. Another criterion encountered on modern ultracentrifuges is that they also have a good, variable range temperature control system. Instruments meeting these criteria were originally called ultracentrifuges, but are now more commonly referred to as analytical ultracentrifuges. Other high-speed centrifuges used in isolation of viruses, nucleic acids, or proteins are referred to as preparative ultracentrifuges. This article will be restricted to analytical ultracentrifugation.

Although many people believe that the ultracentrifuge is restricted to biochemistry or biophysics, this is not the case. This versatile instrument can be applied to colloid chemistry (*3*), to physical chemistry (*3–5*), to polymer chemistry (*3–5*), and to inorganic chemistry (*3–5*). It has been used to study the distribution of radii in colloidal gold sols (*1*, *6*), to determine activity coefficients in silicotungstic acid solutions (*7*) and sucrose (*8*), and also to find the degree of aggregation of various salts in aqueous solutions (*9–13*). In polymer chemistry the ultracentrifuge has been used to measure sedimentation coefficients, average molecular weights, second virial coefficients, and molecular-weight distributions (*5*, *15–24*). Density gradient sedimentation experiments have been used to show that the nitrogen of the deoxyribonucleic acid is divided equally between two subunits which remain intact through many generations (*25*, *26*). The density gradient experiment has also been used to study greases and polymers (*27*, *28*).

Because the subject of analytical ultracentrifugation is so vast, this paper will be restricted to two areas of interest to the authors: self-associations and molecular weight distributions. Both areas were considered early in the development of the ultracentrifuge (*3*), but it has only been in the last few years that real breakthroughs have been made in these areas (*16–24*, *29–35*). Another reason for considering these areas is that they can be studied by other methods (*36*, *37*), chromatography for ex-

ample (*38–41*), so that comparative studies can be made. With self-associations we will show how data from two or more types of experiments can be used to extract more information about the system. For instance, values of the equilibrium constant(s), K_i, and of the monomer concentration, c_1, obtained from sedimentation equilibrium experiments can be used with sedimentation velocity experiments (performed under the same solution conditions) to evaluate the sedimentation coefficient of the associating species (*42*), or they might be used with analytical gel chromatography experiments to extract the partition coefficients (*42*). In molecular weight distribution studies, a comparison can be made with molecular weight distributions obtained from sedimentation equilibrium, sedimentation velocity, and analytical gel chromatography experiments (*20*). Readers interested in these and other areas of ultracentrifugation should consult the various reviews and monographs on the subject cited above.

MOLECULAR-WEIGHT DISTRIBUTIONS

Introduction

The idea of obtaining molecular-weight distributions (MWD) of non-associating, heterogeneous polymer solutions goes back to Rinde (*6*) in 1928. Several methods based on procedures proposed by Rinde were tried with varying success (*4*, *5*, *24*); in some cases experimental error produced negative values for the differential distribution of molecular weights, $f(M)$. Two recent developments, one by Donnelly (*16*, *17*) and one by Scholte (*18–20*), have reopened interest in obtaining MWDs from sedimentation equilibrium experiments; both methods were restricted to ideal, dilute solutions and to cells with sector-shaped centerpieces. These restrictions have recently been removed (*24*), and it has been shown experimentally that one can obtain MWDs from nonideal solutions (*43*, *44*). Good agreement has been observed with the MWD obtained on a dextran sample by analytical gel chromatography and by sedimentation equilibrium experiments after correction for nonideal behavior. In this section we shall describe these developments. More complete details on obtaining MWDs are to be found in papers by Adams et al. (*24*), by Gehatia and Wiff (*23*, *45–49*), by Donnelly (*16*, *17*), and by Scholte (*18–20*).

The Basic Sedimentation Equilibrium Equation

If one assumes that the refractive index increments, ψ_i, and the partial specific volumes, $\bar{v}_i$, for the polymeric components are the same, then one

can obtain the weight-average molecular weight, M_w, or its apparent value, $M_{w\,app}$, from sedimentation equilibrium experiments. The condition of sedimentation equilibrium requires that the temperature, T, be constant and that the total potential, $\bar{\mu}_i$, of component i (*3–5, 24*) be constant at each radial position r, in the solution column of the ultracentrifuge cell. The quantity $\bar{\mu}_i$ is defined by

$$\bar{\mu}_i = \mu_i - \frac{M_i\omega^2 r^2}{2} \tag{1}$$

For component i, μ_i is the molar chemical potential, $-M_i\omega^2r^2/2$ is the centrifugal potential, M_i is the molecular weight, and $\omega = 2\pi(\text{rpm})/60$ is the angular velocity of the rotor. The radial position r is restricted to distances between the position of the air-solution meniscus, r_m, and the position of the cell bottom, r_b, i.e., $r_m \leq r \leq r_b$. It is convenient to define two new quantities (*5, 24*)

$$\Lambda = \frac{(1 - \bar{v}\rho_0)\omega^2(r_b^2 - r_m^2)}{2RT} \tag{2}$$

and

$$\xi = \frac{r_b^2 - r^2}{r_b^2 - r_m^2} \tag{3}$$

Here $\bar{v}$ is the partial specific volume of the solute, ρ_0 is the density of the solvent, and R is the universal gas constant ($R = 8.314 \times 10^7$ ergs/deg-mole). Note that $\xi = 0$ when $r = r_b$, and $\xi = 1$ when $r = r_m$.

The sedimentation equilibrium equation for component i can be written as (*15, 24*)

$$-\Lambda M_i c_i = \frac{dc_i}{d\xi} - \Lambda c_i M_i \sum_k B_{ik}' c_k M_k \tag{4}$$

The quantity B_{ik}' represents a nonideal term; it is defined as

$$B_{ik}' = B_{ik} + \frac{\bar{v}}{1000M_k} \tag{5}$$

Here c_i is the concentration (in grams/liter) of component i at radial position r, i.e., it is c_{ir}. For simplicity the subscript r will usually be dropped. It is assumed in the treatment we are using that the natural logarithm of the activity coefficient of component i can be expressed as (*4, 5, 15, 24*)

$$\ln y_i = M_i \sum_k B_{ik} c_k + \cdots \tag{6}$$

where

$$B_{ik} = \left(\frac{\partial \ln y_i}{\partial c_k}\right)_{T,P,c_{j\neq k}} \tag{7}$$

Most ultracentrifuges are equipped with refractometric (Rayleigh and schlieren) optics. The schlieren optical system gives information proportional to dc/dr vs r, and the Rayleigh optics give information proportional to c vs r. Figure 1 shows the type of patterns produced by the two optical systems. Since the schlieren optical system gives information proportional to dc/dr, we must sum the terms in Eq. (4) over all i solute components. Thus

$$\frac{dc}{d\xi} = \sum_i \frac{dc_i}{d\xi} = -\Lambda c M_{wr} + \Lambda \sum_i \sum_k c_i c_k B_{ik}' M_i M_k \tag{8}$$

Here

$$\frac{dc}{d\xi} = -(r_b^2 - r_m^2)\frac{dc}{d(r^2)} \tag{9}$$

and

$$M_{wr} = \sum_i c_i M_i / \sum_i c_i \tag{10}$$

Equation (8) can be rearranged to give

$$\frac{dc}{d\xi} = \frac{-\Lambda c M_{wr}}{1 + \langle B_{ik}' \rangle_r c M_{wr}} = -\Lambda c M_{wr\,\mathrm{app}} \tag{11}$$

provided $\langle B_{ik}' \rangle_r c M_{wr} < 1$. The quantity $\langle B_{ik}' \rangle_r$ is defined by

$$\langle B_{ik}' \rangle_r = \frac{\sum_i \sum_k c_i c_k M_i M_k B_{ik}'}{\sum_i \sum_k c_i c_k M_i M_k} \tag{12}$$

Instead of having a uniform solution as one has with light scattering or with osmometry, the centrifugal field causes a redistribution of the i polymeric components, which is why $\langle B_{ik}' \rangle_r$ varies with r. This is the term which has caused difficulty in analyzing nonideal polymer solutions by sedimentation equilibrium experiments. An ideal, dilute solution will be defined as one for which $\langle B_{ik}' \rangle_r = 0$. In this case $M_{wr\,\mathrm{app}} = M_{wr}$ and the basic sedimentation equilibrium equation becomes

$$dc/d\xi = -\Lambda c M_{wr} \qquad (\langle B_{ik}' \rangle_r = 0) \tag{13}$$

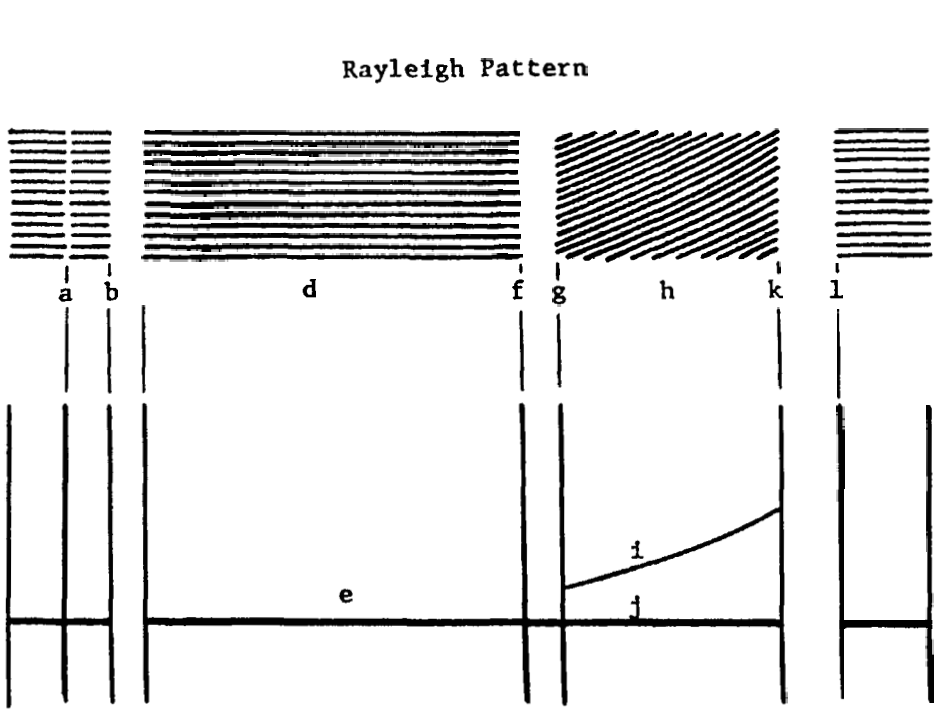

a - reference wire

b - inner index (outer edge)

c - top of cell

d - Rayleigh image from air column (air base line)

e - schlieren image from air column (air base line)

f - air-solvent meniscus

g - air-solution meniscus

h - Rayleigh pattern for solution

i - schlieren pattern for solution

j - solvent base line

k - bottom of cell

l - outer index (inner edge)

FIG. 1. Diagrams of the schlieren (lower) and the Rayleigh interference (upper) patterns obtained from sedimentation equilibrium experiments using double-sector centerpieces.

In order to deal with the $\langle B_{ik}' \rangle_r$ term, it is necessary to make some assumptions. Three cases are described below (*43*).

Case I. Assume that all the $\langle B_{ik}' \rangle$ are equal. For this case $B_{ik}' = B$ and

$$\langle B_{ik}' \rangle_r c_r M_{wr} = B c_r M_{wr} \tag{14}$$

Case II. Assume the speed effect to be small so that it can be ignored, and let $\langle B_{ik}' \rangle_r \cong B_{LS}$, the light scattering second virial coefficient. As the rotor speed goes to zero, the $c_{ir} \rightarrow c_i^0$, the initial concentration of component i. Here B_{LS} is defined by

$$B_{LS} = \frac{\sum_i \sum_k f_i f_k M_i M_k B_{ik}'}{\sum_i \sum_k f_i f_k M_i M_k} \tag{15}$$

and

$$f_i = c_i^0/c_0 \qquad (\text{or } f_k = c_k^0/c_0) \tag{16}$$

is the weight fraction of component i (or k). Note that

$$c_0 = \sum_i c_i^0 \tag{17}$$

Case III. Here a speed effect is included. We assume that

$$\langle B_{ik}' \rangle_r = B_{LS} + \left(\frac{\partial \langle B_{ik}' \rangle_r}{\partial \Lambda^2} \right)_{c_0}^0 \Lambda^2 = B_{LS} + \alpha \Lambda^2 \tag{18}$$

The superscript 0 on the partial derivative means that this quantity is evaluated in the vicinity of $\Lambda = 0$.

How does one evaluate $\langle B_{ik}' \rangle_r$? For the first two cases $\langle B_{ik}' \rangle_r$ is approximated by B_{LS}. Using Donnelly's method (*16*, *17*), if all the B_{ik}' are equal, then there will be no speed effect on the MWD. If there is a speed effect, then there will be a difference in the MWDs determined at two or more speeds. This provides a test for the assumptions. The evaluation of B_{LS} from sedimentation equilibrium experiments has been described in detail by Wan (43) and by Adams et al. (*24*) for ultracentrifuge cells with sector- or nonsector-shaped centerpieces. The methods proposed by Albright and Williams (*15*) can be applied to either type of centerpiece. Essentially the method requires that a series of sedimentation equilibrium experiments be carried out at different speeds (three or more speeds) for each solution. Values of $M_{w\ \text{cell app}}$ are calculated at each speed. These are defined by

$$M_{w\ \text{cell app}} = \frac{c_b - c_m}{\Lambda c_0} \tag{19}$$

for a sector-shaped centerpiece and by

$$M_{w\ \text{cell app}} = -\frac{1}{\Lambda c_0}\int_0^1 \frac{dc}{d\xi}\,dx \tag{20}$$

for a nonsector-shaped centerpiece. The quantity x is the analog of ξ for a nonsector-shaped centerpiece; x is defined as (*24*)

$$x = \frac{\int_{r_m}^{r} f(r)\,dr}{\int_{r_m}^{r_b} f(r)\,dr} \tag{21}$$

Here $f(r)$ is a function that describes how the cross-sectional width of the cell varies with radial distance r. Figure 2 shows the top views of a double-sector centerpiece and of a multichannel equilibrium centerpiece. Once one has run the experiments at different speeds it is necessary to evaluate

$$M^0_{w\ \text{cell app}} = \lim_{\Lambda \to 0} M_{w\ \text{cell app}} = M^0_{w\ \text{app}}$$

This can be done by plotting $M_{w\ \text{cell app}}$ vs Λ and extrapolating the plot to $\Lambda = 0$; such a plot is shown in Fig. 3. The intercept of this plot gives $M^0_{w\ \text{cell app}}$. Alternatively one can plot $\Delta c/c_0$ vs Λ or $-\int_0^1 (dc/d\xi)\,dx/c_0$ vs Λ depending on the type centerpiece one uses (*24*). The limiting slope of these plots as shown in Fig. 4, gives $M^0_{w\ \text{app}}$ for each c_0. Note that these plots must go through the origin; for example, with a sector-shaped centerpiece $\Delta c = 0$ when $\Lambda = 0$. Note also that at constant c_0, $\Delta c/c_0$ is a function of Λ. Thus one could use regression analysis to obtain a polynomial of the form

$$\Delta c/c_0 = \alpha + \beta\Lambda + \gamma\Lambda^2 + \cdots \tag{22}$$

The quantity α should be equal to zero and β can be identified with $M^0_{w\ \text{app}}$.

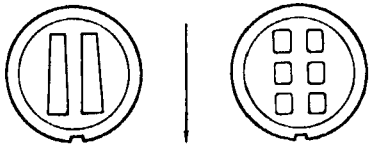

FIG. 2. Top view of double-sector and multichannel equilibrium centerpieces. One side of either centerpiece is reserved for the solvent or buffer solution. The arrow indicates the direction of increasing centrifugal field strength. With multichannel centerpieces the most dilute solution is put in one of the centrifugal or outermost holes, and the most concentrated solution is put in one of the centripetal or innermost holes.

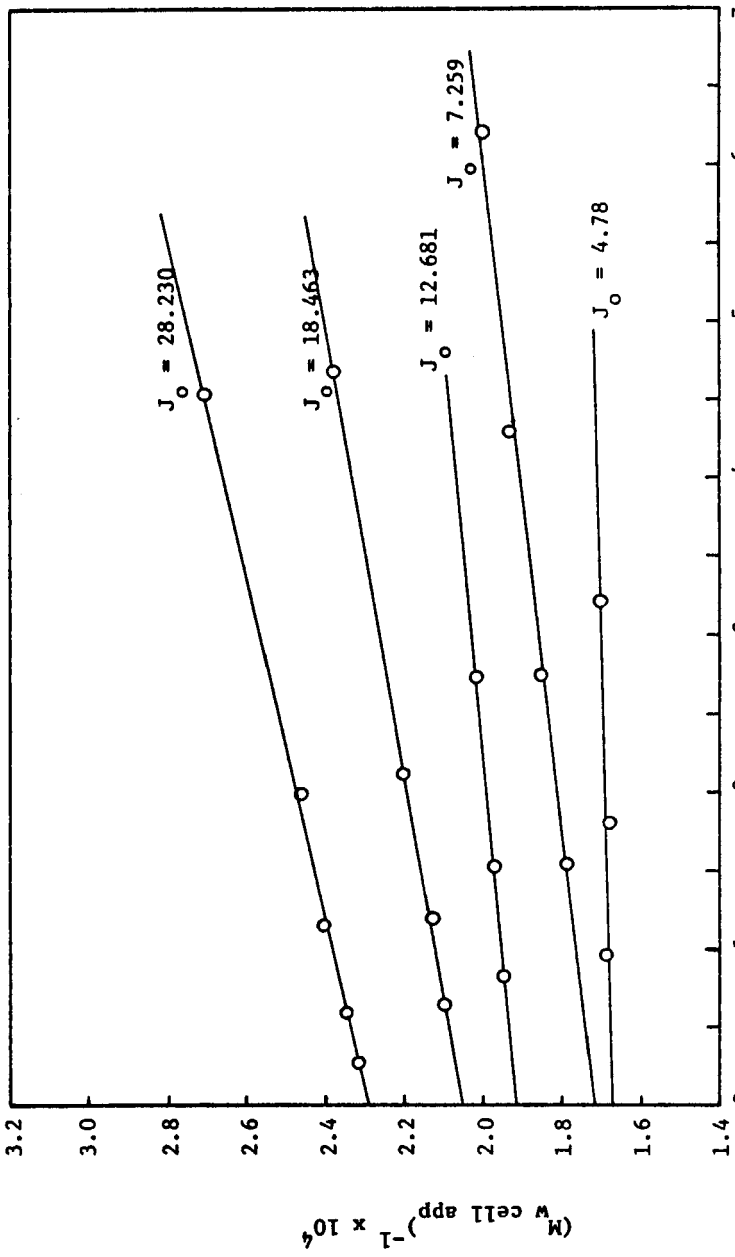

FIG. 3. Plot of $1/M_{w\ cell\ app}$ vs Λ for a dextran T-70 sample dissolved in water ($T = 25\,^{\circ}C$). The initial concentrations, J_0, are given in fringes (12 mm centerpiece, $\lambda = 546$ nm); at 25 °C, $J = 3.297c$ for c in g/l. The intercept of each plot gives $1/M^0_{w\ app}$ for each J_0.

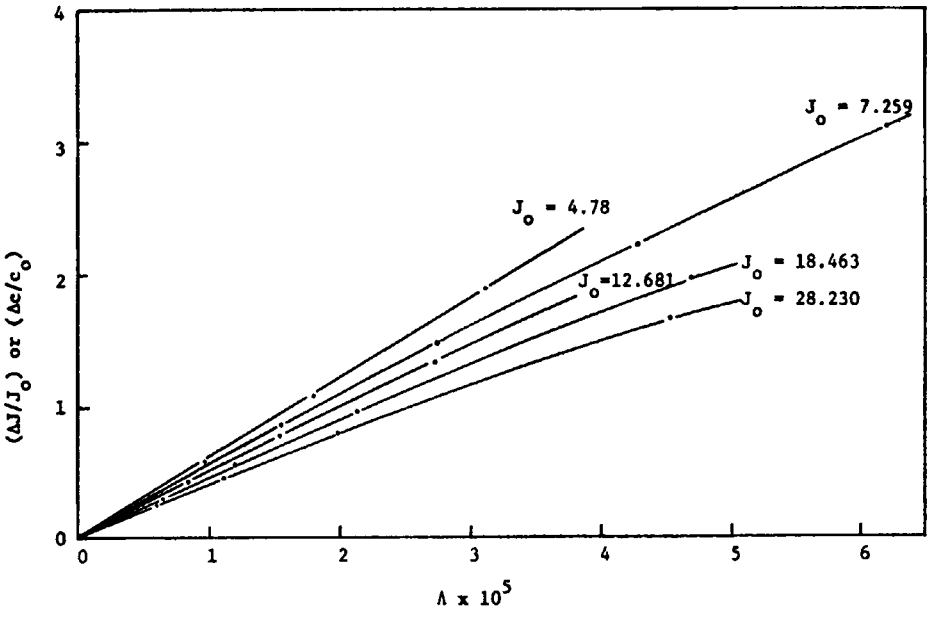

FIG. 4. Plots of $\Delta J/J_0$ vs Λ. The limiting slope of each plot gives $M^0_{w\ app}$. Dextran T-70 dissolved in water. $T = 25°C$.

Fujita (*5*) has shown that the sedimentation equilibrium second virial coefficient, $\langle B_{ik}' \rangle$, depends on Λ^2. With the use of Eq. (18) one notes that at constant $\overline{c_0}$,

$$\lim_{\Lambda \to 0} 1/M_{w\ cell\ app} = \lim_{\Lambda \to 0} \left[\frac{1}{M_w} + (B_{LS} + \alpha\Lambda^2)c_0 + \cdots \right] = 1/M_w + B_{LS}c_0 = 1/M^0_{w\ app} \tag{23}$$

and that

$$\lim_{\Lambda \to 0} \frac{\partial}{\partial \Lambda^2}\bigg|_{c_0} (1/M_{w\ cell\ app}) = \alpha c_0 \tag{23a}$$

Equation (23a) shows how one might try to evaluate α. The quantity B_{LS} is obtained from the slope of a plot of $1/M^0_{w\ app}$ vs c_0 (see Eq. 23); a plot of this kind is shown in Fig. 5. Thus the required quantities for the non-ideal correction can be evaluated from the experimental data. Having an estimated value of the $\langle B_{ik}' \rangle_r$, it is possible to calculate ideal values of c

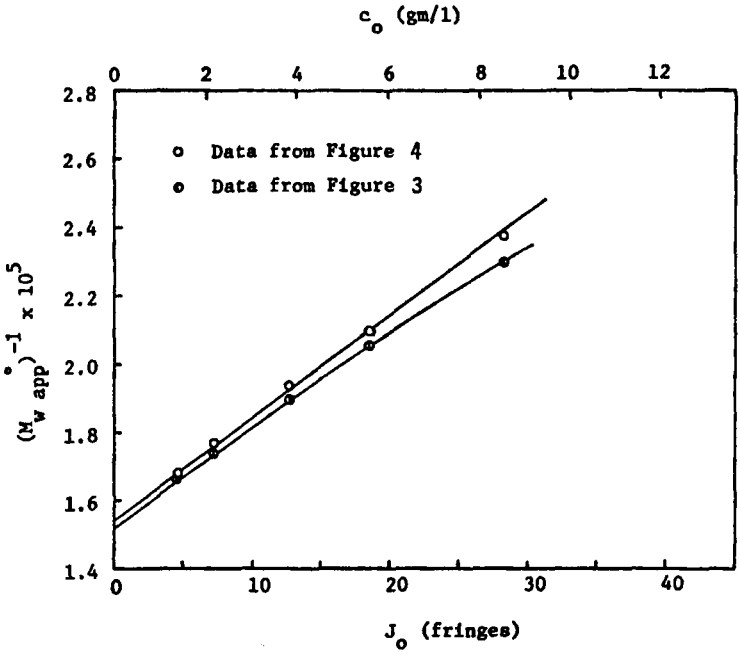

FIG. 5. Plots of $1/M^0_{w\,app}$ vs J_0 for the dextran T-70 sample using data from Figs. 3 and 4. The intercept of this plot gives $1/M_w$. The average value of M_w is 6.59×10^4 Daltons.

or dc/dr (*24*). Equation (11) can be rearranged to give

$$\frac{1}{cM_{wr}} \equiv \frac{-1}{(dc/d\xi)_{\text{ideal}}} = \frac{1}{cM_{wr\,\text{app}}} - \frac{\langle B_{ik}' \rangle_r}{\Lambda} \tag{24}$$

The values of $(dc/d\xi)_{\text{ideal}}$ so obtained can be used with Scholte's method or any of the other methods for obtaining MWDs. For Donnelly's method the quantity $(d \ln c/d\xi)_{\text{ideal}}$ is needed. Thus Eq. (11) can be rearranged to give

$$\frac{1}{M_{wr}} \equiv \frac{-1}{\left[\frac{1}{\Lambda}\frac{d \ln c}{d\xi}\right]_{\text{ideal}}}$$

$$= \frac{1}{M_{wr\,\text{app}}} - \langle B_{ik}' \rangle_r c \tag{24a}$$

Here

$$-\frac{1}{\Lambda}\frac{d\ln c}{d\xi} = M_{wr\ \mathrm{app}} \tag{25}$$

An additional quantity required for Donnelly's method is $c_0/[c(\xi = 1)]_{\mathrm{ideal}}$. This is readily obtained from

$$\frac{c_0}{c(\xi = 1)_{\mathrm{ideal}}} = \int_0^1 \left[\frac{c(\xi)}{c(\xi = 1)}\right]_{\mathrm{ideal}} d\xi \tag{26}$$

Note that

$$\int_1^{\xi} \left(\frac{d\ln c}{d\xi}\right)_{\mathrm{ideal}} d\xi = \ln\left[\frac{c(\xi)}{c(\xi = 1)}\right]_{\mathrm{ideal}} \tag{27}$$

Concentration and Concentration Gradient Distributions

One of the unique features of the sedimentation equilibrium experiment is that it allows the evaluation of average molecular weights without any prior knowledge of the MWD. In addition it is also possible to obtain the MWD from sedimentation equilibrium experiments. No other physical method for studying macromolecules has this versatility. We have shown in the previous section how nonideal effects can be accounted for, so it will be assumed that nonideal corrections have been applied, and in the discussion that follows equations applicable to ideal dilute solution conditions will be used.

For ideal, dilute solution conditions, Eq. (4) becomes (*4, 5, 24*)

$$\frac{d\ln c_i}{d\xi} = -\Lambda M_i \tag{28}$$

This equation can be integrated between $\xi = 1$ and $\xi = \xi$ and then recast in exponential form to give

$$c_i(\xi) = c_i(\xi = 1)\exp\left[-\Lambda M_i \xi\right] \tag{29}$$

From Eq. (29) one notes that the concentration distribution for component i is in exponential form. Different values of M_i will give different concentration distributions and also different concentration gradient distributions; thus one will expect different values for any average molecular weight at any radial position. The weight average molecular weight at any radial position, M_{wr}, is given by Eq. (13) or its more familiar form (*3–5, 24, 50*)

$$\frac{d\ln c}{d(r^2)} = AM_{wr} \tag{30}$$

where

$$A = (1 - \bar{v}\rho)\omega^2/2RT \tag{31}$$

The z-average molecular weight at any radial position, M_{zr}, is obtained from (*3*, *50*)

$$M_{zr} = \frac{d(cM_{wr})}{dc} = M_{wr} + c\frac{dM_{wr}}{dc} \tag{32}$$

Here

$$M_{zr} = \frac{\sum_i c_{ir}M_i^2}{\sum_i c_{ir}M_i} \tag{33}$$

In principle it is possible to obtain any higher average molecular weight, since (*3–5*, *24*, *50*)

$$M_{(z+q)r} = \frac{d(cM_wM_zM_{z+1}\cdots M_{(z+q-1)})_r}{d(cM_wM_zM_{z+1}\cdots M_{(z+q-2)})_r} \tag{34}$$

Note that

$$M_{(z+q)r} = \frac{\sum c_{ir}M_i^{(q+2)}}{\sum c_{ir}M_i^{(q+1)}} \qquad q = 0, 1, 2, \ldots \tag{35}$$

In practice it is virtually impossible to go beyong M_{zr}, since numerical differentiation is involved. The number-average molecular weight at any radial position, M_{nr}, is not readily obtainable, since (*50*, *51*)

$$\frac{c_r}{M_{nr}} - \frac{c_{rm}}{M_{nr_m}} = A\int_{r_m}^{r} cd(r^2) \tag{36}$$

Here two unknowns, M_{nr} and M_{nr_m}, are involved. Even though this equation can be transformed to one equation in one unknown, it is still difficult to obtain M_{nr_m} (*50*).

The quantities M_{wr} and M_{zr} are useful in the analysis of self-association; they can also be used to develop methods for the evaluation of the cell averages $M_{w\,\text{cell}}$ and $M_{z\,\text{cell}}$. For nonassociating polymers in ideal, dilute solutions, one can obtain the M_w and M_z of the polymer from measurements of $M_{w\,\text{cell}}$ and $M_{z\,\text{cell}}$. In order to evaluate $M_{w\,\text{cell}}$ or $M_{z\,\text{cell}}$, it is necessary to know the shape of the cell (centerpiece), since the conservation of mass equations enter into these equations. The conservation of mass states that the total amount of solute in a closed system is constant at any time. The mass of solute is given by (*4*, *5*, *24*, *50*)

$$\text{mass solute} = \int_{r_m}^{r_b} c_r\, dV \tag{37}$$

Sector-Shaped Centerpieces

For a sector-shaped centerpiece

$$dV = \frac{\theta h}{2} d(r^2) \tag{38}$$

where θ is the sector angle and h is the cell thickness. The amount of solute at the beginning of the experiment is given by

$$\text{mass solute} = \frac{\theta h}{2} c_0(r_b^2 - r_m^2) \tag{39}$$

and at sedimentation equilibrium it is given by

$$\text{mass solute} = \frac{\theta h}{2} \int_{r_m}^{r_b} c_r \, d(r^2) \tag{40}$$

Setting Eqs. (39) and (40) equal to each other, one obtains (*3, 5, 24*)

$$c_0(r_b^2 - r_m^2) = \int_{r_m}^{r_b} c_r \, d(r^2) \tag{41}$$

or

$$c_0 = \int_0^1 c(\xi) \, d\xi \tag{41a}$$

In order to evaluate c_m, the meniscus concentration, one must note that

$$(c_0 - c_m)(r_b^2 - r_m^2) = \int_{r_m}^{r_b} (c_r - c_m) \, d(r^2) \tag{42}$$

The quantity $c_r - c_m$ is the difference in concentration between the concentration at r and that at r_m; it is directly proportional to the difference in Rayleigh interference fringes between these two radial positions. The quantity $M_{w\,\text{cell}}$ is defined by (*3–5, 24, 51*)

$$M_{w\,\text{cell}} = \frac{\int_{r_m}^{r_b} M_{wr} c \, d(r^2)}{\int_{r_m}^{r_b} c_r \, d(r^2)} \tag{43}$$

Since $cM_{wr} = \sum_i c_{ir} M_i$, one notes that

$$\begin{aligned} M_{w\,\text{cell}} &= \frac{\sum_i M_i \int_{r_m}^{r_b} c_i \, d(r^2)}{c_0(r_b^2 - r_m^2)} \\ &= \frac{\sum_i M_i c_i^0 (r_b^2 - r_m^2)}{c_0(r_b^2 - r_m^2)} = \frac{\sum_i c_i^0 M_i}{\sum_i c_i^0} \\ &= M_w \text{ of the original solution} \end{aligned} \tag{44}$$

The insertion of Eq. (30) into the numerator of Eq. (43) leads to

$$M_{w\ \mathrm{cell}} = \frac{\int_{r_m}^{r_b} \frac{d \ln c}{d(r^2)}\, c\, d(r^2)}{Ac_0(r_b^2 - r_m^2)} = \frac{c_b - c_m}{\Lambda c_0}$$
$$[\Lambda = A(r_b^2 - r_m^2)] \tag{45}$$

The quantity $M_{z\ \mathrm{cell}}$ is defined by (*3–5, 24, 51*)

$$M_{z\ \mathrm{cell}} = \frac{\int_{r_m}^{r_b} M_{zr}\, dc}{\int_{c_m}^{c_b} dc} = \frac{\left[\left(\frac{1}{r}\frac{dc}{dr}\right)_{r_b} - \left(\frac{1}{r}\frac{dc}{dr}\right)_{r_m}\right]}{2A(c_b - c_m)} \tag{46}$$

Here M_{zr} is given by (*20*)

$$M_{zr} = \frac{1}{2A}\frac{d\left(\frac{1}{r}\frac{dc}{dr}\right)}{dc} \tag{47}$$

One can use arguments similar to those used in Eq. (44) to show that $M_{z\ \mathrm{cell}}$ is the M_z of the polymer. For nonideal solutions one obtains $M_{w\ \mathrm{app}}$ and $M_{z\ \mathrm{app}}$ from Eqs. (45) and (46). It can be shown that as $\Lambda \to 0$, $M_{w\ \mathrm{app}} \to M^0_{w\ \mathrm{app}}$, where

$$M^0_{w\ \mathrm{app}} = \frac{M_{w\ \mathrm{cell}}}{1 + B_{LS}c_0 M_{w\ \mathrm{cell}}} \tag{48}$$

A similar relation can be developed for $M_{z\ \mathrm{app}}$ (*24, 43*).

Nonsector-Shaped Centerpieces

With nonsector-shaped centerpieces dV is given by

$$dV = hf(r)\, dr \tag{49}$$

and the conservation of mass equation (see Eq. 37) becomes (*3, 24*)

$$c_0 \int_{r_m}^{r_b} f(r)\, dr = \int_{r_m}^{r_b} c_r f(r)\, dr \tag{50}$$

or using dx (see Eq. 21)

$$c_0 = \int_0^1 c(\xi)\, dx \tag{51}$$

To evaluate c_m it is noted that

$$(c_0 - c_m)\int_{r_m}^{r_b} f(r)\, dr = \int_{r_m}^{r_b} (c_r - c_m) f(r)\, dr \tag{52}$$

or using dx

$$(c_0 - c_m) = \int_0^1 [c(\xi) - c(\xi = 1)]\, dx \tag{53}$$

The quantity $M_{w\ \mathrm{cell}}$ is defined by (*4*, *18*)

$$M_{w\ \mathrm{cell}} = \frac{\int_{r_m}^{r_b} M_{wr} c_r f(r)\, dr}{\int_{r_m}^{r_b} c_r f(r)\, dr} = \frac{\dfrac{1}{2A}\displaystyle\int_{r_m}^{r_b} \frac{f(r)\, dc}{r}}{c_0 \displaystyle\int_{r_m}^{r_b} f(r)\, dr} = \frac{-1}{\Lambda c_0}\int_0^1 \frac{dc}{d\xi}\, dx \tag{54}$$

If the solution is nonideal, then Eq. (54) gives $M_{w\ \mathrm{app}}$. The limit of $M_{w\ \mathrm{app}}$ as $\Lambda \to 0$ becomes $M^0_{w\ \mathrm{app}}$, which is defined by Eq. (48). The quantity $M_{z\ \mathrm{cell}}$ is defined by (*13*, *50*)

$$M_{z\ \mathrm{cell}} = \frac{\displaystyle\int_{r_m}^{r_b} M_{zr} f(r) \frac{dc}{r}}{\displaystyle\int_{r_m}^{r_b} f(r) \frac{dc}{r}} = \frac{\dfrac{1}{2A}\displaystyle\int_{r_m}^{r_b} \frac{f(r)}{r}\left[d\left(\frac{1}{r}\frac{dc}{dr}\right)\Big/ dc\right] dc}{\displaystyle\int_{r_m}^{r_b} \frac{f(r)}{r}\, dc} \tag{55}$$

Donnelly's Method for MWDs (16, 17)

This method is based on data obtained from a single sedimentation equilibrium experiment. It is quite good with unimodal MWDs, but it may not be as good as Scholte's method with multimodal MWDs. The starting equation here is Eq. (29). In order to make it more useful, it is necessary to relate c_i ($\xi = 1$) to the initial concentration of i, c_i^0; this requires the application of the conservation of mass equation. Thus this method must be considered separately for each of the two kinds of centerpieces.

Sector-Shaped Centerpieces

For component i the conservation of mass equation becomes

$$c_i^0 = \int_0^1 c_i(\xi)\, d\xi \tag{56}$$

The insertion of Eq. (29) in Eq. (56) and subsequent rearrangement leads to

$$c_i(\xi = 1) = \frac{\Lambda M_i c_i^0}{1 - \exp(-\Lambda M_i)} \tag{57}$$

The substitution of Eq. (57) into Eq. (29) yields

$$c_i(\xi) = \frac{\Lambda M_i c_i^0 \exp(-\Lambda M_i \xi)}{1 - \exp(-\Lambda M_i)} \tag{58}$$

Summation over the i solute components followed by division of both sides by c_0 leads to (*16, 17, 24, 50*)

$$\theta(\xi) = \frac{c(\xi)}{c_0} = \sum_i \frac{\Lambda M_i f_i \exp(-\Lambda M_i \xi)}{1 - \exp(-\Lambda M_i)} \tag{59}$$

Here $f_i = c_i^0/c_0$ is the weight fraction of component i. Equation (59) can be differentiated with respect to ξ to give

$$\begin{aligned} -\theta'(\xi) &= \frac{-1}{c_0}\frac{dc(\xi)}{d\xi} = \sum_i \frac{\Lambda^2 M_i^2 f_i \exp(-\Lambda M_i \xi)}{1 - \exp(-\Lambda M_i)} \\ &= U(\Lambda, \xi) \end{aligned} \tag{60}$$

Equations (59) and (60) are used in Scholte's (*18–20*) method. Now if one assumes that a continuous distribution of molecular weights is present, then f_i is replaced by $f(M)\,dM$ which is the weight fraction of solute having molecular weights between M and $M + dM$, and the summation is replaced by an integral running between 0 and ∞. Thus Eqs. (59) and (60) become (*16, 17, 24, 50*)

$$\theta(\xi) = \int_0^\infty \frac{\Lambda M f(M) \exp(-\Lambda M \xi)\, dM}{1 - \exp(-\Lambda M)} \tag{61}$$

and

$$\theta'(\xi) = -\frac{1}{c_0}\frac{dc(\xi)}{d\xi} = \int_0^\infty \frac{\Lambda^2 M^2 f(M) \exp(-\Lambda M \xi)\, dM}{1 - \exp(-\Lambda M)} \tag{62}$$

Here $f(M)$ is the differential distribution of molecular weights; this is the quantity we want to determine. Donnelly pointed out that Eqs. (61) and (62) are Laplace transforms (*16, 17*); if one can find an analytical expression for the Laplace transform, then the MWD can be obtained from the inverse of the Laplace transform. In order to see this more clearly, in Eq. (16) let $\xi = s$, $t = \Lambda M$, and

$$\phi(t) = \frac{\Lambda M f(M)}{1 - \exp(-\Lambda M)} = \frac{t f(M)}{1 - \exp(-t)} \tag{63}$$

Then it follows that

$$L\{\phi(t)\} = \Lambda\theta = \int_0^\infty \phi(t)e^{-st}\,dt = f(s) \tag{64}$$

Here $L\{\phi(t)\}$ is the symbol for the Laplace transform of the function $\phi(t)$. In order to use $L\{\phi(t)\}$, we must find an analytical expression for it; in other words, what is the form of $f(s)$? Donnelly solved this neatly (*16*, *17*, *24*). Let us define

$$F(n, u) = \frac{1}{\left(\dfrac{d \ln c}{d(r^2)}\right)} \tag{65}$$

where

$$u = \frac{r^2 - r_m^2}{r_b^2 - r_m^2} = 1 - \xi = 1 - s \tag{66}$$

Suppose that one makes a plot of $F(n, u)$ vs u, and suppose that this plot is a straight line of the form

$$F(n, u) = P - Qu \tag{67}$$

Here P is the intercept at $u = 0$ and Q is the slope. Now note that

$$du = \frac{d(r^2)}{r_b^2 - r_m^2} \tag{68}$$

or

$$d(r^2) = (r_b^2 - r_m^2)\,du = b\,du \tag{68a}$$

The integral

$$\int_{r_m}^{r} \frac{d \ln c}{d(r^2)}\,d(r^2) = \ln \frac{c_r}{c_{r_m}} = \ln \frac{c(\xi)}{c(\xi = 1)} \tag{69}$$

and

$$\exp \int_{r_m}^{r} \frac{d \ln c}{d(r^2)}\,d(r^2) = \frac{c(\xi)}{c(\xi = 1)} \tag{70}$$

If Eq. (70) is multiplied by $\Lambda c(\xi = 1)/c_0 = 1/K$, then we obtain $\Lambda\theta(\xi)$. Thus

$$\begin{aligned} L\{\phi(t)\} = \Lambda\theta(\xi) &= \frac{\Lambda c(\xi = 1)}{c_0} \exp \int_{r_m}^{r} \frac{d \ln c}{d(r^2)}\,d(r^2) \\ &= \frac{1}{\mathrm{K}} \exp \int_{r_m}^{r} \frac{d \ln c}{d(r^2)}\,d(r^2) = \frac{1}{K} \exp \int_0^u \frac{b\,du}{F(n, u)} \end{aligned} \tag{71}$$

The insertion of Eqs. (65) and (68a) into Eq. (69) leads to

$$\int_{r_m}^{r} \frac{d \ln c}{d(r^2)} d(r^2) = \int_0^u \frac{b\, du}{F(n, u)} \tag{72}$$

Since $F(n, u) = P - Qu$, one notes that

$$\int_0^u \frac{b\, du}{P - Qu} = \frac{b}{Q} \ln \frac{P}{P - Qu} \tag{73}$$

Using Eq. (66) this becomes

$$\frac{b}{Q} \ln \frac{P}{P - Qu} = \frac{b}{Q} \ln \frac{P}{Q[(P/Q) - 1 + s]} \tag{73a}$$

Therefore

$$\begin{aligned} L\{\phi(t)\} &= \Lambda\theta = \frac{1}{K}\left[\frac{P}{Q\{(P/Q) - 1 + s\}}\right]^{b/Q} \\ &= \frac{(P/Q)^{b/Q}}{K}\left[\frac{1}{s + a}\right]^n \end{aligned} \tag{74}$$

where $a = (P/Q) - 1$ and $n = b/Q$.
A well-known mathematical relation states that (*16*, *17*, *24*)

$$\frac{\Gamma(n)}{(s + a)^n} = \int_0^\infty t^{n-1} e^{-(s+a)t}\, dt \tag{75}$$

where $\Gamma(n)$ is the gamma function of n. Thus it follows that

$$\begin{aligned} L\{\phi(t)\} &= \int_0^\infty \phi(t) e^{-st}\, dt \\ &= \int_0^\infty \frac{(P/Q)^{b/Q}}{K} \frac{t^{(b/Q)-1}}{\Gamma(b/Q)} \exp\{-[(P/Q) - 1]t - st\}\, dt \end{aligned} \tag{76}$$

Comparison of the two integrals in Eqs. (75) and (76) indicates that

$$\phi(t) = \frac{(P/Q)^{b/Q}}{K} \frac{t^{(b/Q)-1}}{\Gamma(b/Q)} e^{-[(P/Q)-1]t} \tag{77}$$

It follows from Eq. (63) that

$$f(M) = \frac{(P/Q)^{b/Q}}{K} \frac{t^{(b/Q)-2}}{\Gamma(b/Q)} e^{-[(P/Q)-1]t}(1 - e^{-t}) \tag{78}$$

Nonsector-Shaped Centerpieces (24, 43)

Here the conservation of mass equation for component i is (*24*, *43*)

$$c_i^0 = \int_0^1 c_i \, dx \tag{79}$$

The insertion of Eq. (29) into Eq. (79) leads to

$$c_i(\xi = 1) = \frac{c_i^0 \exp(-\Lambda M_i \xi)}{\int_0^1 [\exp(-\Lambda M_i \xi)] \, dx} \tag{80}$$

The analogs of Eqs. (59) and (60) become (*24*, *43*)

$$\hat{\theta}(\xi) = \frac{c(\xi)}{c_0} = \sum_i \frac{f_i \exp(-\Lambda M_i \xi)}{\int_0^1 [\exp(-\Lambda M_i \xi)] \, dx} \tag{81}$$

and

$$\begin{aligned} -\hat{\theta}'(\xi) &= \frac{-1}{c_0} \frac{dc(\xi)}{d\xi} = \sum_i \frac{\Lambda M_i f_i \exp(-\Lambda M_i \xi)}{\int_0^1 [\exp(-\Lambda M_i \xi)] \, dx} \\ &= V(\Lambda, \xi) \end{aligned} \tag{82}$$

For a continuous distribution of molecular weights, $\hat{\theta}(\xi)$ becomes

$$\hat{\theta}(\xi) = \int_0^\infty \frac{f(M) \exp(-\Lambda M \xi) \, dM}{\int_0^1 [\exp(-\Lambda M \xi)] \, dx} \tag{83}$$

Letting $t = \Lambda M$, $\xi = s$, and

$$\gamma(t) = \frac{f(M)}{\int_0^1 [\exp(-\Lambda M \xi)] \, dx} \tag{84}$$

one can show that the Laplace transform, $L\{\gamma(t)\}$, of $\gamma(t)$ is given by (*24*, *43*)

$$\Lambda \hat{\theta}(\xi) = L\{\gamma(t)\} = \int_0^\infty \gamma(t) e^{-st} \, dt \tag{85}$$

Now we can follow the previous procedure. $F(n, u)$ (see Eq. 65) is defined in the same manner, and Eq. (71) applies to this case also. So, if $F(n, u) = P - Qu$, then $L\{\gamma(t)\}$ will also be defined by Eq. (74). However, $f(M)$ in this case becomes

$$f(M) = \frac{(P/Q)^{b/Q}}{K} \frac{t^{(b/Q)-1}}{\Gamma(b/Q)} e^{-[(P/Q)-1]t} \int_0^1 [\exp(-\Lambda M \xi)] \, dx \tag{86}$$

Thus the only difference in the two methods is that

$$f(M) = \left[\frac{1 - \exp(-\Lambda M)}{\Lambda M}\right]\phi(t) \tag{87}$$

for a sector-shaped centerpiece, and

$$f(M) = \left\{\int_0^1 \exp(-\Lambda M\xi)\, dx\right\}\gamma(t) \tag{88}$$

for a nonsector-shaped centerpiece. Table I in the paper by Adams et al. (*24*) gives the Laplace transform for three different equations for $F(n, u)$; a fourth case is described by Donnelly. For other situations not covered by these four cases, one might be able to use the complex inversion method to find the inverse of the Laplace transform. Although the mathematical treatment may look formidable, this is really a beautiful and simple method to use.

Results with Donnelly's Method

Figure 6 shows plots of $F(n, u)$ vs u (see Eq. 65) for a dextran sample dissolved in water. The sedimentation equilibrium experiments were run at 25°C and at 8000 rpm. The upper plot has not been corrected for

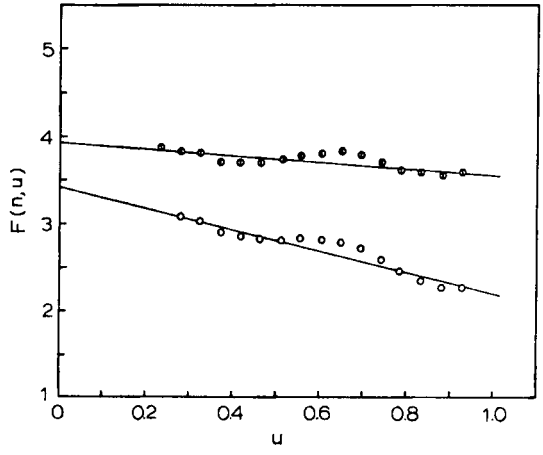

FIG. 6. Plot of $F(n, u)$ vs u for Dextran T-70 in water. $T = 25$ °C. This plot is required for Donnelly's method for obtaining MWDs. These experiments were carried out in multichannel, equilibrium centerpieces. The upper plot (①) uses data uncorrected for nonideal behavior, whereas the lower plot (○) uses data corrected for nonideal behavior assuming $B_{LS} = \langle B_{ik}' \rangle_r$.

nonideality, whereas the lower plot has been corrected for nonideality. We then assumed $\langle B_{ik}' \rangle_r \equiv B_{LS}$, where B_{LS} was calculated from experiments at different speeds. Equation (20) was used to calculate $M_{w\ \text{cell app}}$ at each speed. These results were extrapolated to zero speed, and B_{LS} was determined from a plot of $1/M^0_{w\ \text{app}}$ vs c_0 (see Eq. 24). The value of B_{LS} used to obtain $(d \ln c/d\xi)_{\text{ideal}}$ (see Eq. 24a) was 0.322×10^{-6} for concentrations in terms of green (12 mm) fringes. With the aid of Eqs. (26) and (27), one could proceed with the analysis described in the preceding section for nonsector-shaped cells. Figure 7 shows the MWD obtained by Donnelly's method with sector- and nonsector-shaped cells. Note that the corrected values agree with the manufacturer's MWD which was obtained by a combination of analytical gel chromatography and light scattering. Also note that the uncorrected MWDs in no way resemble the corrected or manufacturer's MWD. Figure 6 shows the difference in corrected and uncorrected plots of $F(n, u)$ vs u; the correction makes quite a difference in the MWD.

Scholte's Method (18–20)

This method is based on Eq. (60) for a sector-shaped centerpiece or Eq. (82) for a nonsector-shaped centerpiece and requires that one perform sedimentation equilibrium experiments at different speeds on the same solution. After the Rayleigh and schlieren data have been recorded at one speed, the speed is changed, and the solution is allowed to come to sedimentation equilibrium again; the photographic data are collected at each new speed before going on to the next speed. This method uses the field to fractionate the sample. At lower speeds the concentration distribution of the lower molecular weight solutes is relatively smaller than that for the high molecular weight solutes. At higher speeds the larger molecular weight solutes are pushed toward the cell bottom and the lower molecular weight solutes are distributed throughout the cell.

Sector-Shaped Centerpieces

The starting equation here is Eq. (60). Scholte designates the derivative as $U(\Lambda, \xi)$; thus he writes (*18–20, 24*)

$$\begin{aligned} U(\Lambda, \xi)_j &= -\frac{1}{c_0}\frac{dc(\xi)}{d\xi} \\ &= \sum_i f_i \frac{\Lambda_j{}^2 M_i{}^2 \exp(-\Lambda_j M_i \xi)}{1 - \exp(-\Lambda_j M_i)} + \delta_j \\ &= \sum_i f_i K_{ij} + \delta_j \end{aligned} \tag{89}$$

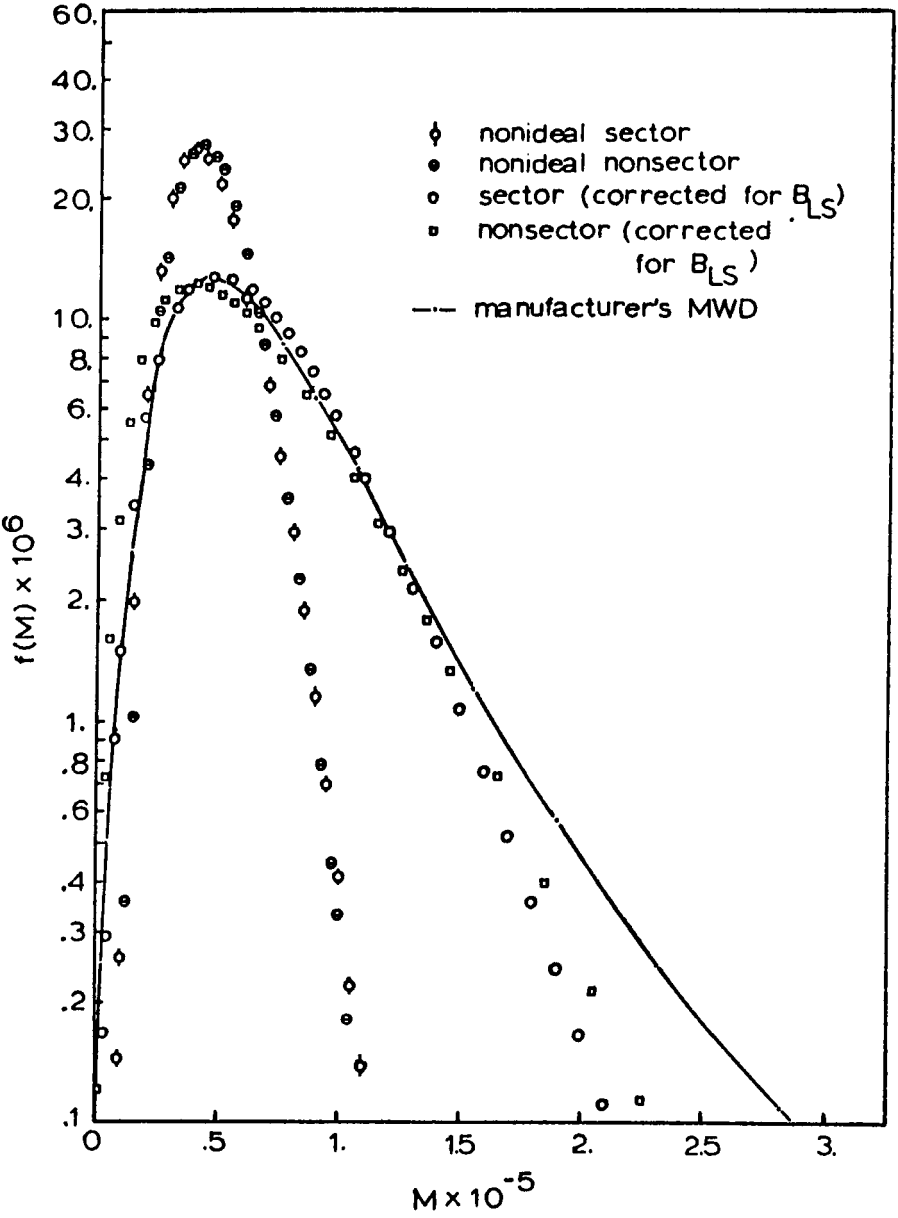

FIG. 7. MWD for the Dextran T-70 sample by Donnelly's method with and without the B_{LS} correction for nonideality. Note how much better the corrected data agrees with the manufacturer's MWD (solid line), which was obtained by analytical gel chromatography. An even better agreement is obtained when a rotor speed correction is included. The data in these plots were collected using sector- and nonsector-shaped centerpieces.

where

$$K_{ij} = \frac{\Lambda_j^2 M_i^2 \exp(-\Lambda_j M_i \xi)}{1 - \exp(-\Lambda_j M_i)} \tag{90}$$

and δ_j is a term expressing experimental error. The quantities subscripted by i depend on the molecular weights, M_i, that are chosen; thus f_i will be the weight fraction of component i whose molecular weight is M_i. The quantity Λ_j has the subscript j to indicate that this quantity depends on the speed used and not on the molecular weight of component i. The experimental data are usually read at five evenly spaced values of ξ, i.e., at $\xi = 0$, 1/4, 1/2, 3/4, and 1, although at some speeds one will not be able to read data at all of the values of ξ. In order to use Scholte's method (*18–20*), one must assume a discrete range of molecular weights, M_i, which will bracket the sample. For example, the molecular weights chosen for this first range or first series might be $M_1 = 2{,}500$, $M_2 = 5{,}000$, $M_3 = 10{,}000$, and so on until a molecular weight larger than the largest expected value for the polymer is attained. It was found by experience that the interval between molecular weights is logarithmic, and that the series is best constructed so that each successive molecular weight chosen has twice the value of the molecular weight immediately preceeding it. The speeds chosen should be such that the ratio of successive ω^2 is two, or as close to this ratio as possible. The values of $U(\Lambda, \xi)$ that are available should exceed the number of M_i that are chosen. The first choice of molecular weights is called the first series. Once the first series is chosen, the $U(\Lambda, \xi)$ values can be used to write down a set of linear equations.

$$\begin{aligned}
U(\Lambda, \xi)_1 &= f_1 K_{11} + f_2 K_{21} + f_3 K_{31} + \cdots + \delta_1 \\
U(\Lambda, \xi)_2 &= f_1 K_{12} + f_2 K_{22} + f_3 K_{32} + \cdots + \delta_2 \\
&\vdots \qquad\quad \vdots \qquad\quad \vdots \qquad\quad \vdots \\
U(\Lambda, \xi)_n &= f_1 K_{1n} + f_2 K_{2n} + f_3 K_{3n} + \cdots + \delta_n
\end{aligned} \tag{91}$$

Scholte (*18–20*) solves this set of equations by a linear programming technique. These equations are perfectly adapted to linear programming, since (1) we are dealing with a set of linear equations involving only positive quantities; (2) $\sum_i f_i = 1$, i.e., the sum of all the weight fractions must be one; (3) each f_i must satisfy the condition $0 \leq f_i \leq 1$; and (4) the f_i's are chosen so the sum of the absolute value of the error is a minimum, i.e., $\sum_j |\delta_j|$ is a minimum. The f_i are determined on a computer.

The set of f_i obtained from the computer program for the first series of molecular weights is not unique. One could choose another set of M_i's, and this is just what Scholte does. A second series of M_i is obtained by

multiplying each M_i in the first series by $2^{1/4}$, i.e., M_i(2nd series) $= 2^{1/4} \times M_i$(1st series). Another array of $U(\Lambda, \xi)_j$ is set up for the second series, and again the computer is used to obtain the f_i using the linear programming technique. This procedure is repeated with a third series, M_i(3rd series) $= 2^{1/2} \times M_i$(1st series), and a fourth series, M_i (4th series) $= 2^{3/4} \times M_i$(1st series). Table 1 shows an example of the type of data used and the results obtained from the computer program for the first and third series. This data is taken from the work of Scholte (*18*). The material used was a polyethylene sample which was dissolved in biphenyl; the experiments were performed at the theta temperature, 123.2°C. Figure 8 shows the MWD that was obtained; note that Scholte plots his MWD as $Mf(M)$ vs M. It is quite evident from this figure that Scholte's method can detect a multimodal MWD.

How does one obtain the MWD? First of all note that

$$\sum_i f_i \text{ (any series)} = 1 \tag{92}$$

$$\sum_i f_i \text{ (all four series)} = 4 \tag{92a}$$

and

$$\sum_i f_i/4 \text{ (for all four series)} = 1 \tag{92b}$$

Thus Eq. (92b) is also a solution, and it could be used in obtaining the plot of $f(M)$ vs M since more points would be available. In order to obtain a plot of $f(M)$ vs M note that

$$\sum_i f_i \text{ (any series)} = 1 = \int_0^\infty f(M)\, dM \tag{93}$$

TABLE 1a
Tabulation of Raw Data Needed for Molecular Weight Distribution

	ξ^a				
$\Lambda \times 10^6$	0	1/4	1/2	3/4	1
2.5	0.294	0.260	0.232	0.208	0.187
10	2.121	1.237	0.799	0.554	0.405
40			1.346	0.639	0.372
160			0.959	0.337	0.144

[a]Note that $\Lambda = (1 - \bar{v}\rho)\omega^2(r_b^2 - r_m^2)/2RT$.

$$\xi = \frac{r_b^2 - r^2}{r_b^2 - r_m^2}$$

$\xi = 0$ when $r = r_b$.

$\xi = 1$ when $r = r_m$.

TABLE 1b
Results Obtained from Computer Program[a]

First series			Third series		
M_i	f_i	$M_i^2 f(M)_i$	M_i	f_i	$M_i^2 f(M)_i$
8,839	0	0	12,450	0	0
17,678	0.031	790.8	24,900	0.075	2,694.81
35,356	0.084	4,285.6	49,800	0.149	10,707.36
70,712	0.313	31,937.7	99,600	0.453	65,106.49
141,424	0.450	91,833.8	199,200	0.291	83,646.75
282,848	0.104	42,447.6	398,400	0.011	6,323.81
565,696	0	0	796,800	0.012	13,797.40
1,131,392	0.015	24,489.0	1,593,600	0.009	20,696.10
2,262,784	0.0021	6,856.9	3,187,200	0.0002	919.83
Σf_i	0.9991		Σf_i	1.0002	

[a]For the second series (not tabulated): M_i(2nd series) = M_i(1st series) $\times 2^{1/4}$. For the third series: M_i(3rd series) = M_i(1st series) $\times 2^{1/2}$. For the fourth series: M_i(4th series) = M_i(1st series) $\times 2^{3/4}$.

Note that

1. Σf_i(1st series) = 0.9991.
2. Σf_i(2nd series) = 1.002.
3. $$\int_0^\infty Mf(M)\frac{dM}{M} = 1 \simeq \Delta \ln M \, \Sigma[Mf(M)]_i$$
$$= \frac{0.693}{4} \sum_{\text{all 4 series}} \frac{f_i}{0.693}$$
4. $$M_w = \int_0^\infty Mf(M)dM = \int_0^\infty M^2 f(M)\frac{dM}{M}$$
$$\simeq \Delta \ln M \sum_{\text{all 4 series}} [M^2 f(M)]_i$$
$$= \frac{0.693}{4} \sum_{\text{all 4 series}} \frac{M_i f_i}{0.693}$$

Using data from the first and third series

$$\Delta \ln M = \frac{0.693}{2} = 0.346 = \frac{1}{2}\ln 2$$
$$\Sigma[M^2 f(M)]_i = 406{,}533.96$$

By the trapezoidal rule

$$M_w = 140{,}661 \simeq \frac{0.693}{2} \times 406{,}533.96$$

Scholte obtained 141,000 from the MWD
141,000 from experiments at different speeds
142,000 from measurements at one speed

Sample: Polyethylene L-30-76. Solvent: Biphenyl. Temperature: 123.2°C (theta temperature).

Data taken from Scholte's papers (*18*, *19*).

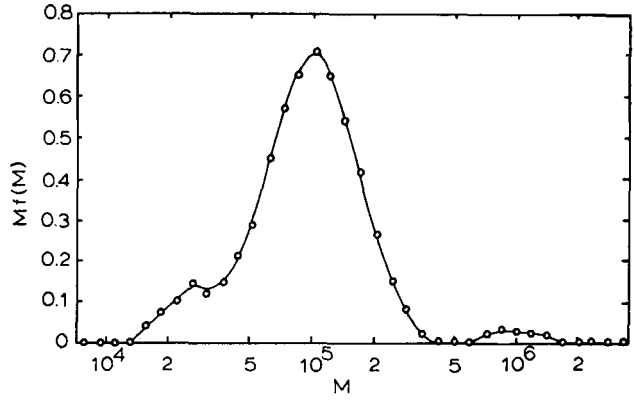

FIG. 8. Scholte's method for MWDs. This is a plot of $Mf(M)$ vs M for polyethylene dissolved in biphenyl at the theta temperature (123.2°C). Redrawn from the data obtained by Scholte (*18*, *19*).

Thus the area under the curve for the plot of $f(M)$ vs M must be 1. Clearly we cannot plot f_i vs M_i, even if the intervals between successive molecular weights, ΔM, is constant, since the area under this curve would be ΔM. We could plot $f_i/\Delta M$ (for one series) vs ΔM or $f_i/4\Delta M$ vs ΔM (for data from all four series). But, now note that the interval between successive molecular weights is $2^{1/4}$, i.e., $M_j = M_i 2^{1/4}$. Therefore, Scholte (*18–20*) suggested that the following procedure be used.

$$\sum_i \frac{f_i}{4}(\text{all four series}) = 1 = \int_0^\infty f(M)\,dM$$

$$= \int_0^\infty Mf(M)\frac{dM}{M} \simeq \Delta \ln M \sum_i [Mf(M)]_i \qquad (94)$$

Since $\Delta \ln M_i$ is constant and equal to (1/4) ln 2 or 0.693/4, then

$$\sum_i [Mf(M)]_i = \frac{4}{0.693} \qquad (95)$$

Since $\sum_i f_i$ (all four series) = 4, one notes that for all four series

$$\sum_i \frac{f_i}{0.693} = \frac{4}{0.693} \qquad (96)$$

Thus

$$[Mf(M)]_i = f_i/0.693 \qquad (96a)$$

So, if one plots $Mf(M)$ vs ln M, where $\Delta \ln M = \ln M_j - \ln M_i = 0.693/4$, then the area under the curve is 1. This is how Scholte obtained the curve shown in Fig. 8.

Nonsector-Shaped Centerpieces (24, 43)

The starting equation here is Eq. (82), which can be written as

$$V(\Lambda, \xi)_j = \sum_i \frac{\Lambda_j M_i f_i \exp(-\Lambda_j M_i \xi)}{\int_0^1 [\exp(-\Lambda_j M_i \xi)]\, dx} + \delta_j$$
$$= \sum_i f_i H_{ij} + \delta_j \tag{97}$$

where

$$H_{ij} = \frac{\Lambda_j M_i \exp(-\Lambda_j M_i \xi)}{\int_0^1 [\exp(-\Lambda_j M_i \xi)]\, dx} \tag{98}$$

and δ_j is the experimental error. Clearly one can set up an array of $V(\Lambda, \xi)$ in the same manner as one does with the $U(\Lambda, \xi)$ (see Eqs. 91), choose a range of molecular weights, and solve for the f_i's by linear programming. Thus the analysis is done in the same manner as before. Note that for each choice of M_i, the integral in Eq. (98) must be evaluated numerically; the easiest way to do this is to use a computer.

Scholte has also modified his method so that instead of minimizing the sum of the absolute value of the error, one minimizes the square of the error. Results using both procedures give excellent agreement (*20*).

The Method of Gehatia and Wiff (23, 45–49)

Gehatia and Wiff have developed a very elegant method of determining MWDs from a single sedimentation equilibrium experiment; they claim to be able to analyze multimodal distributions. Figure 9 shows the results obtained with a simulated MWD; the solid line represents the true value and the circles represent the computed distribution. Their method was originally developed for ideal, dilute solution conditions and for sector-shaped centerpieces. Their starting equation is Eq. (61), which they write as (*23*)

$$U(\xi) = \int_0^\infty K(\xi, M) f(M)\, dM = \int_0^{M_{max}} K(\xi, M) f(M)\, dM \tag{99}$$

Here

$$K(\xi, M) = \frac{\Lambda M \exp(-\Lambda M \xi)}{1 - \exp(-\Lambda M)} \tag{100}$$

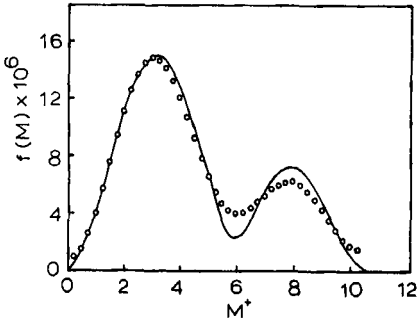

FIG. 9. The Gehatia and Wiff method for MWDs. This is a simulated example (*23*). The $M^+ = M/13{,}953$. The solid curve represents the true distribution. The open circles represent calculated values of $f(M)$ vs M^+.

M_{max} is the largest molecular weight in the MWD; beyond M_{max}, $f(M) = 0$. They point out that equations of the type shown by Eq. (99) are improperly posed problems in the Hadamard sense. What this means is that small errors in $U(\xi)$ can cause severe oscillations when one attempts to obtain $f(M)$ from this integral equation. A way to avoid this problem is to use a regularizing function which dampens out the oscillations. Although their model was originally set down for cells with sector-shaped centerpieces, it could also be applied to cells with nonsector-shaped centerpieces. In this case Eq. (83) would be used, and it would be written as

$$V(\xi) = \int_0^{\infty} H(\xi, M) f(M)\, dM = \int_0^{M_{max}} H(\xi, M) f(M)\, dM \quad (101)$$

where

$$H(\xi, M) = \frac{\Lambda M \exp(-\Lambda M \xi)}{\int_0^1 [\exp(-\Lambda M \xi)]\, dM} \quad (102)$$

The Gehatia-Wiff method need not be restricted to ideal, dilute solution conditions. Our methods for correcting for nonideal behavior, or a method proposed by Gehatia and Wiff (*45*, *49*) for nonideal solutions, could be used. Their method does require the use of a computer. For more details the reader should consult the papers by Gehatia and Wiff (*23*, *45–49*).

Molecular-Weight Distributions from Sedimentation Velocity Experiments

The sedimentation velocity experiment can also be used to obtain MWDs. Much of the pioneering work in the determination of MWDs

from sedimentation velocity experiments was done by Prof. J. W. Williams of the University of Wisconsin-Madison and his associates (*4*, *5*, *24*, *52*). The advantage of the technique is its rapidity; it takes about 2 hr to do one sedimentation velocity experiment. The disadvantages of the method are (1) its tediousness, (2) the fact that the theory is more empirical and not on as rigorous a foundation as the sedimentation equilibrium method, and (3) that two (sometimes three) extrapolations are involved. Nevertheless, there is an extensive literature on MWDs from sedimentation velocity experiments or on differential distributions of sedimentation coefficients, $g(s)$, which can be transformed to MWDs if a relation between s and M is known (*4*, *5*, *24*, *52–57*). With the advent of automatic plate readers (*58*), the tediousness associated with this method can be alleviated, and the availability of pulsed lasers and multiplexers may allow three to five (depending on the rotor type) experiments to be performed simultaneously.

The differential distribution of sedimentation coefficients, $g(s)$, is defined by (*4*, *5*, *43*, *52*, *53*)

$$g(s) = \frac{1}{c}\frac{dc}{ds} = \frac{dG(s)}{ds} \tag{103}$$

Here $G(s)$ is the integral distribution of sedimentation coefficients; it is defined by (*4*, *5*, *43*, *52*, *53*)

$$G(s) = \int_0^s g(s)\,ds = \sum_i r^2\tilde{n}_{0i}/r_m{}^2\tilde{n}_0 \tag{104}$$

The quantity $\tilde{n}_0 = n - n_0$ is the refractive index difference between solution (n) and solvent (n_0); $\tilde{n}_{0i}$ is the refractive index difference for component i. In these equations c is the concentration of the macromolecular solutes, s is the sedimentation coefficient, r is the radial position in the moving boundary, and r_m is the radial position of the air–solution meniscus. If the refractive index increments, ψ_i, of the macromolecular components are all the same, then $n - n_0 = \psi c$, and $G(s)$ becomes

$$G(s) = \sum_i r^2 c_{0i}/r_m{}^2 c_0 \tag{105}$$

Equation (103) for $g(s)$ is often written in a more useful form, namely, (*4*, *5*, *43*, *52*, *53*)

$$g(s) = \frac{r^3\omega^2 t}{c_0 r_m{}^2}\left(\frac{\partial c}{\partial r}\right)_t \tag{106}$$

Here we have used the relations

$$c = c_0(r_m/r)^2 \tag{107}$$

$$\frac{dc}{ds} = \frac{dc}{dr}\frac{dr}{ds} \tag{108}$$

and

$$\frac{dr}{ds} = \frac{d}{ds}(r_m \exp[s\omega^2 t])$$
$$= t\omega^2 r_m \exp(s\omega^2 t) = r\omega^2 t \tag{109}$$

Since both sedimentation and diffusion occur in a moving boundary, the experimentally measured $g(s)$ is actually an apparent value, $g^*(s)$, which is also defined by Eq. (106). The spreading of the moving boundary due to sedimentation (s) is proportional to t, while the spreading of the boundary due to diffusion (D) is proportional to $t^{1/2}$ (*5*, *59*). If the diffusion effects are not too great, there should be an intermediate region of time in which values of $g^*(s)$ and $1/t$ are linearly correlated. Thus extrapolation of $g^*(s)$ to $1/t = 0$ should eliminate diffusion effects; values of $g^*(s)$ at $1/t = 0$ are designated by $g^\circ(s)$. With nonaqueous solutions, pressure effects are important, and a correction must also be made for them. For details on these corrections, consult the reviews by Williams et al. (*4*), Baldwin and Van Holde (*53*), or the monograph by Fujita (*5*).

Once $g^\circ(s)$ has been obtained, it is necessary to remove concentration dependence so that the true $g(s)$ can be obtained. There are several ways to solve this problem(s). In one method, introduced by Baldwin et al. (*3*, *60*, *61*), values of $g^\circ(s)/g^\circ_{max}(s)$ at infinite time are obtained for each boundary gradient curve at a certain initial concentration c_0. Here $g^\circ_{max}(s)$ is the maximum value of $g(s)$. Then one extrapolates $1/s$ to c_0 at each fixed value of $g^\circ(s)/g^\circ_{max}(s)$ for all of the sedimentation velocity experiments at various initial concentrations. This procedure gives s_0, the sedimentation coefficient at zero concentration, for each ratio of $g^\circ(s)/g^\circ_{max}(s)$. One obtains $1/g^\circ_{max}(s)$ from (*5*, *60*, *61*)

$$1/g^\circ_{max}(s) = \int_0^\infty [g^\circ(s)/g^\circ_{max}(s)]\, ds \tag{110}$$

Once $g^\circ_{max}(s)$ is known, then it is a simple matter to obtain $g^\circ(s_0)$. A plot of $g^\circ(s_0)$vs s_0 gives the plot of the differential distribution of sedimentation coefficients. The integral distribution of sedimentation coefficients, $G(s_0)$, is obtained from Eq. (104). Figure 10 shows a plot of $g^\circ(s_0)$ vs s_0 and $G^\circ(s_0)$ vs s_0 for a gelatin sample (*60*).

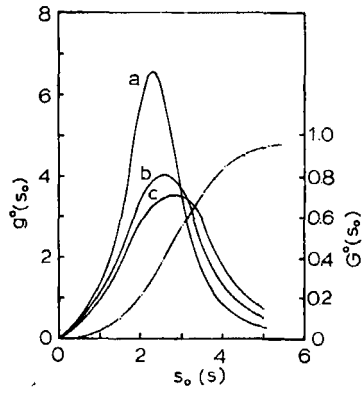

FIG. 10. Differential, $g^\circ(s)$ and integral, $G^\circ(s_0)$, distributions of sedimentation coefficients for a gelatin sample (*60*). The Gaussian Curves a, b, and c represent values of $g^\circ(s)$ at $c = 0.746$ g/dl (a), at $c = 0.306$ g/dl (b), and at $c = 0$ (c). The integral distribution (— ·), $G^\circ(s_0)$, is obtained by numerical integration of Curve c.

In order to obtain a differential distribution of molecular weights, $f(M)$, one has to have an empirical relation of the form (*4*, *5*, *43*)

$$s_0 = KM^\alpha \tag{111}$$

or

$$s_0 = KM_w^\alpha \tag{111a}$$

The constants K and α depend on the temperature and the polymer–solvent combination. This relation can be established by measuring the sedimentation coefficients and molecular weights (M) or weight-average molecular weights (M_w) of some polymer fractions or some samples of the same type polymer. Values of K and α for many polymers are tabulated in the *Polymer Handbook* (*14*). If one lets $g^\circ(s_0)\, ds_0$ be the weight fraction of polymer having a sedimentation coefficient (at infinite dilution) between s_0 and $s_0 + ds_0$, then because of Eqs. (111) and (111a) one notes that

$$g^\circ(s_0)\, ds_0 = f(M)\, dM \tag{112}$$

and

$$f(M) = g^\circ(s_0)\frac{ds_0}{dM} = \frac{\alpha s_0 g^\circ(s_0)}{M} \tag{113}$$

Figure 11 shows a plot of $f(M)$ vs M for a trimodal polystyrene sample

obtained at the theta temperature, 34.2°C, in cyclohexane by sedimentation equilibrium (top) and by sedimentation velocity (bottom) experiments. Note the excellent agreement in the two techniques; the data are taken from the paper by Scholte (*20*). Table 2 shows the values of M_n, M_w, and M_z obtained by the two ultracentrifugal techniques and by gel permeation chromatography (*20*). The agreement between the methods is quite good, demonstrating the versatility of the ultracentrifuge in this area.

Concluding Remarks

By far the most commonly used method for obtaining a MWD is the gel permeation method, which was developed by Moore (*62*) for the rapid determination of MWDs of thermoplastics. Many more recent details about gel permeation chromatography will be found in the book edited by Ezrin (*63*). This book contains the proceedings of a conference on Polymer

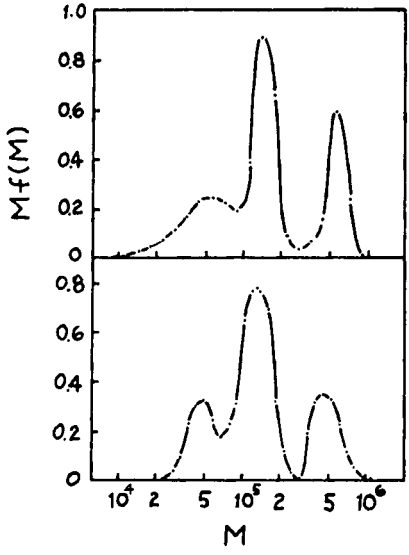

FIG. 11. Plots of $Mf(M)$ vs M for a trimodal blend of polystyrene. The upper curve was obtained from sedimentation velocity experiments using $g^*(s_0)$; the lower curve was obtained from sedimentation equilibrium experiments using Scholte's linear programming method (*20*). Values of M_n, M_w, and M_z for this sample obtained by various methods are listed in Table 2.

TABLE 2
Average Molecular Weights of a Blend of Three Polystyrene Samples

	How obtained	$M_n \times 10^3$	$M_w \times 10^3$	$M_z \times 10^3$
1.	From average molecular weights of the original samples	102	204	385
2.	From sedimentation equilibrium experiments by Scholte's method (Eq. 59) using linear programming	106	202	362
3.	From sedimentation velocity experiments [$g(s)$]	101	205	365
4.	From gel permeation chromatography	96	204	439

Molecular Weight Methods; about one-third of the papers in the book deal with gel permeation chromatography. We have seen in Fig. 7 that there is good agreement with the MWD of the dextran sample determined from sedimentation equilibrium experiments (*43*, *44*) and by a combination of analytical gel chromatography and light scattering. The details of the manufacturer's method for obtaining the MWD of the dextran sample are given in the papers by Granath (*64*, *65*). We have also seen in Table 2 that there is good agreement between ultracentrifugal methods for obtaining MWDs and gel permeation chromatography. The agreement between the various methods is gratifying.

The ultracentrifuge has been used for the characterization of latex particles (*66*, *67*). Electron microscopy established that the particles were spherical. The latex particles are large compared to the wavelength of the blue (λ = 456 nm) or the green (λ = 546 nm) lines of mercury, so that the particles undergo Mie scattering. Thus a photoelectric scanner could be used to obtain sedimentation coefficients, s, and $g^\circ(s_0)$, thediffere ntial distribution of sedimentation coefficients. From the Stokes-Einstein relation s could be related to x^2, the square of the radius of the particles; hence, a distribution of radii could also be obtained. Here is a beautiful example of a practical application of the ultracentrifuge, since it could be used for quality control.

Wales and Rehfeld (*55*) have related the intrinsic viscosity, $[\eta]$, and $g^\circ(s_0)$ for linear polymers. Their procedure has been used by Merle and Sarko (*56*) and by Bluhm and Sarko (*57*) to obtain a polydispersity index, i.e., a ratio of M_w/M_n, in addition to $g(s_0)$ for some synthetic, linear, stereo-regular polysaccharides.

Automatic plate readers have been developed for reading Rayleigh fringes (*58*). Modulatable lasers are available now; in fact we are using them ourselves. Multihole rotors (4 to 6 holes) are also available so that 3 to 5 sedimentation velocity or 3 to 15 sedimentation equilibrium experiments (3 to 5 for a sector-shaped centerpiece or 9 to 15 for a multichannel equilibrium centerpiece) can be performed in the same time it takes to perform one experiment. An interferometric optical system which gives refractive index gradients as a family of fringes has been developed by Bryngdahl and Ljunggren (*68*); it is used on the Christ Omega II ultracentrifuge. The patterns produced by this optical system (*68*), the Rayleigh optical system, and perhaps the schlieren optical system could be analyzed with automatic plate readers. The output from the plate reader could be fed into a computer. Thus the tediousness associated can be removed. Ultracentrifugal analysis for heterogeneity, homogeneity, or MWDs should have an interesting future.

SELF-ASSOCIATIONS

Introduction

Chemical equilibria of the type

$$nP_1 \rightleftarrows P_n, \quad n = 2, 3, \ldots \tag{114}$$

$$nP_1 \rightleftarrows qP_2 + mP_3 + \cdots \tag{115}$$

and related equilibria involving a solute P are known as self-associations. These reactions are widely encountered. Among materials that undergo self-association are many proteins (*30–32*, *35*, *40*), soaps and detergents (*69–72*), purine (*33*, *73*), and nucleosides and nucleotides (*33*, *74*, *75*) as well as some polymers (*76*). The existence of self-associations was recognized early in the development of the ultracentrifuge (*3*). The first theoretical treatment of self-associations by sedimentation equilibrium was by Tiselius (*77*); no methods for analyzing self-associations were presented in his paper. The next development was by Debye who showed how the micellar aggregation of soaps and detergents could be studied by light scattering (*69*); this treatment can be applied to sedimentation equilibrium experiments. Steiner developed a very elegant method for analyzing self-associations by light scattering (*78*) or by osmotic pressure (*79*). Some of his procedures were applied to the Archibald method (an ultracentrifugal technique related to sedimentation equilibrium experiments) by Rao and Kegeles (*80*) and were used by them to study the self-association of α-chymotrypsin in phosphate buffer.

Up to this point the analysis of self-associations was restricted to ideal, dilute solutions. Adams and Fujita (*81*) first showed how to analyze a nonideal self-association; their treatment was restricted to a monomer–dimer association. Adams and Williams (*82*) extended the analysis to monomer–*n*-mer associations beyond dimer ($n \geq 3$); they introduced the apparent weight fraction of monomer, f_a, into the analysis. Subsequently Adams (*29*) discovered an interrelation between the number- (M_{nc}) and weight- (M_{wc}) average molecular weights (or their apparent values in nonideal solutions). He showed how other self-associations besides monomer–*n*-mer associations could be analyzed. Since then new improvements in the method of analyzing self-associations have been developed. Chun et al. (*34*) introduced a graphical procedure for studying nonideal monomer–*n*-mer and indefinite self-associations; their method makes the analysis much neater and simpler. Another method for analyzing self-associations was developed by Derechin (*83*, *84*) who used the multinomial theorem. More recently Šolc and Elias (*85*) have studied the theory for heterogeneous self-associations; this is an area still in its infancy.

In the study of self-associations one is often dealing with multicomponent systems. With an associating protein one may need a buffer to control the pH, plus some supporting electrolytes, such as NaCl or KCl, to swamp out charge effects. Thus one has three or more components—the associating solute, the supporting electrolyte, water, and sometimes buffers. Vrij and Overbeek (*86*) and also Casassa and Eisenberg (*87*) showed that if a solution containing an ionizable, macromolecular solute was dialyzed against a solution containing supporting electrolyte and/or buffers, then the sedimentation equilibrium, light-scattering, or osmotic pressure equations reduce to a form that is formally identical to the equations for a two-component system. Heretofore most studies on ionizable, self-associating solutes have been restricted to larger molecules such as proteins, but the recent development of hollow fiber dialyzers with a low molecular weight cut-off (200 Daltons) now allows the study of small, ionizable solutes. In this section the equations for a two-component system will be used. The equilibrium constant(s), K_i, the second virial coefficient, BM_1, the partial specific volume, $\bar{v}$, and the refractive index increment, ψ, refer to constituents defined by the Vrij-Overbeek (*86*) or Casassa-Eisenberg (*87*) conventions.

Conditions for Simultaneous Chemical and Sedimentation Equilibrium

At constant temperature the condition for chemical equilibrium for

reactions described by Eqs. (114) and (115) is (*30*, *81*)

$$n\mu_1 = \mu_n, \qquad n = 2, 3, \ldots \tag{116}$$

Here $\mu_i (i = 1, 2, \ldots)$ is the molar chemical potential of associating species i. The condition for sedimentation equilibrium requires that the total potential, $\bar{\mu}_i$, for each constituent be constant everywhere in the cell. $\bar{\mu}_i$ is defined by Eq. (1). For self-associations one notes that

$$\begin{aligned} M_2 &= 2M_1 \\ M_3 &= 3M_1 \end{aligned} \tag{117}$$

or

$$M_j = jM_1$$

Using Eqs. (1), (116), and (117), it can be shown for self-associating solutes that

$$n\bar{\mu}_1 = \bar{\mu}_n = \text{constant} \tag{118}$$

at sedimentation equilibrium ($n = 2, 3, \ldots$). This means that the total molar potential of constituent i has the same relation that the chemical potential has when self-association is present.

Assumptions Required for the Analysis of Self-Associations

In order to analyze self-associations it is necessary to make the following assumptions (*29–35*, *81*): (a) The partial specific volumes, $\bar{v}$, of all the associating solutes are the same, or the density increments, $(\partial\rho/\partial c)_\mu$, are the same for all associating solutes. (b) The refractive index increments, ψ, of the associating species are equal. (c) The natural logarithm of the activity coefficient, y_i, on the c-scale (grams/liter) can be represented by

$$\ln y_i = iBM_1c, \qquad i = 2, 3, \ldots \tag{119}$$

Here B is a constant that is characteristic of the solute–solvent mixture; BM_1 is known as the second virial coefficient. It has been shown in light-scattering experiments on mercaptalbumin and its mercury dimer that Eq. (119) is valid (*88*). Furthermore, in his study of the self-association of organic dyes, Braswell (*89*) pointed out that in its limiting form the Debye-Hückel theory indicates that the mean ionic activity coefficients have a similar relation, i.e.,

$$\gamma_\pm(\text{dimer}) = \gamma_\pm{}^2(\text{monomer}) \tag{120}$$

Another reason for using Eq. (119) is that it makes the analysis easier,

since K_i and BM_1 can be evaluated from experimentally available data. If the ψ and $\bar{v}$ or $(\partial\rho/\partial c)_\mu$ differ for each constituent, then one does not obtain M_{wc} and the analysis becomes more formidable.

As a consequence of Eq. (119), the concentration of species n can be expressed as (*29–35, 81*)

$$c_n = K_n c_1^{\,n} \tag{121}$$

and the total concentration, c, of the associating solute is given by

$$c = c_1 + K_2 c_1^{\,2} + \cdots + K_j c_1^{\,j} + \cdots \tag{122}$$

The second virial coefficient, BM_1, does appear in the expressions for the apparent average molecular weights and for the apparent weight fraction of monomer.

It has been shown that one cannot use $M_{w\,\mathrm{cell}}$ (see Eq. 45) in the analysis of self-associations; instead the quantity M_{wr} (see Eq. 30) must be used. Adams and Fujita (*81*) showed that M_{wr} or its apparent value, $M_{wr\,\mathrm{app}}$, are functions of the total solute concentration, c, for self-associations. Thus the symbols M_{wc} and M_{wa} will be used in place of M_{wr} and $M_{wr\,\mathrm{app}}$; the subscript c will indicate that we are dealing with a self-association. For self-associating solutes the basic sedimentation equilibrium equation becomes (*29–35, 81*)

$$\frac{d\ln c}{d(r^2)} = AM_{wa} = \frac{AM_{wc}}{(1 + BM_{wc}c)} \tag{123}$$

Here

$$A = (1 - \bar{v}\rho)\omega^2/2RT \tag{124}$$

or

$$A = 1000(\partial\rho/\partial c)_\mu \omega^2/2RT \tag{125}$$

and

$$\frac{M_1}{M_{wa}} = \frac{M_1}{M_{wc}} + BM_1 c \tag{126}$$

For an ideal, dilute solution, $BM_1 = 0$ and $M_{wa} = M_{wc}$.

In order to analyze self-associations it is necessary to do experiments with a series of solutions of different initial concentrations, c_0. Sedimentation equilibrium experiments are performed on each solution, and for each solution one can obtain values of M_{wa} vs c ($c = c_r$). These values of M_{wa} vs c for each experiment are pieced together to make a plot of M_{wa} vs c as shown in Fig. 12. Here the different symbols indicate results obtained

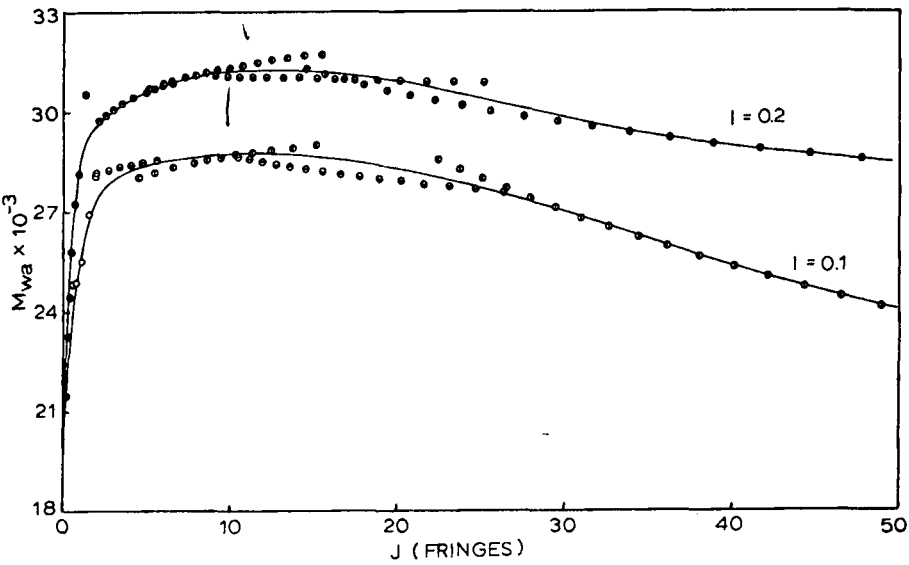

FIG. 12. Self-association of β-lactoglobulin C in glycine buffers at 10°C. Both buffers had 0.2 *M* glycine and 0.1 *M* HCl (pH 2.46 at 23.5°C). The second buffer had 0.1 *M* KCl in addition so that its ionic strength was 0.2. In both cases nonideal behavior is observed, and a monomer–dimer association appears to be present (*104*). At 25°C, $J = 3.394c$ for c in g/l ($\lambda = 632.8$ nm; 12 mm centerpiece).

with solutions of different initial concentrations; remember that $M_{wa} = f(c)$ for self-associations. A smooth curve is drawn through the M_{wa} vs c plot, and the plot is extrapolated to M_1, the monomer molecular weight. In principle one should be able to extrapolate values of M_{wa} or $M_{wa}(1 - \bar{v}\rho)$ to zero concentration so that the correct value of M_1 or $M_1(1 - \bar{v}\rho_0)$ required by the Vrij-Overbeek (*86*) or Casassa-Eisenberg (*87*) conventions is obtained. In actual practice one is forced to choose a value of M_1 from amino acid analysis or some other method, since with strong associations the plots of M_{wa} vs c or $1/M_{wa}$ vs c become quite steep in the vicinity of zero concentration.

Relation Between M_{wa}, M_{na}, and $\ln f_a$. Applicability to Light Scattering and Osmometry

From the smooth plot of M_{wa} vs c a plot of M_1/M_{wa} vs c can be constructed. A minimum in this plot (or a maximum in the plot of M_{wa} vs c)

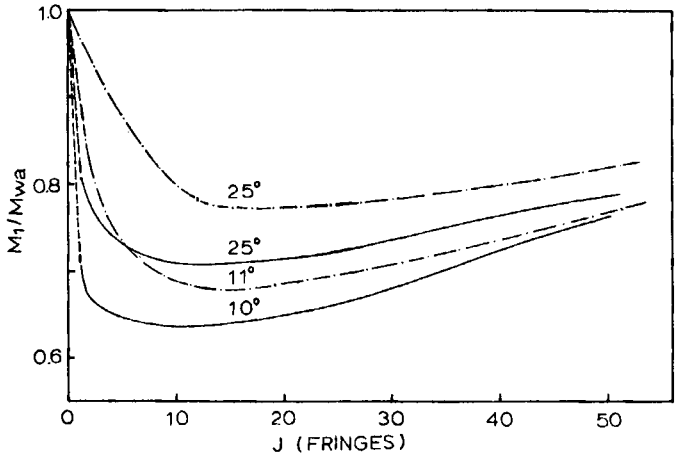

FIG. 13. Self-association of β-lactoglobulins A (— ·) and C(——) in 0.2 *M* glycine buffer (pH 2.46 at 23.5°C; ionic strength 0.1). Note the temperature effect on the self-association. Also note that β-lactoglobulin C undergoes a stronger monomer-dimer self-association than does the A variant. Both proteins exhibit nonideal behavior under these solution conditions. These genetic variants differ by three amino acids. The concentrations are given in red fringes (12 mm centerpieces; $\lambda = 632.8$ nm); at 25°C, $J = 3.394c$ for c in g/l (*35*, *104*).

is indicative that a nonideal self-association is present. Figure 13 shows such a plot. From plots of M_1/M_{wa} vs c one can obtain M_{na} (*29*, *30*), the apparent number-average molecular weight, and $\ln f_a$ (*30*, *82*), the natural logarithm of the apparent weight fraction of monomer. The quantity M_1/M_{na} is obtained from

$$\frac{M_1}{M_{na}} = \frac{1}{c}\int_0^c \frac{M_1}{M_{wa}}\,dc \tag{127}$$

where

$$\frac{M_1}{M_{na}} = \frac{M_1}{M_{nc}} + \frac{BM_1c}{2} \tag{128}$$

The quantity $\ln f_a$ is obtained from

$$\ln f_a = \int_0^c \left(\frac{M_1}{M_{wa}} - 1\right)\frac{dc}{c} \tag{129}$$

where

$$\ln f_a = \ln f_1 + BM_1c \tag{130}$$

and

$$f_1 = c_1/c \tag{131}$$

is the weight fraction of monomer. Note that the

$$\lim_{c\to 0}\left(\frac{M_1}{M_{wa}} - 1\right)\Big/ c$$

exists, so that the lower limit of the integral is zero. If dimer is present, the limit is $-K_2 + BM_1$, and if dimer is absent the limit is BM_1. Since M_{wa} can be obtained from light-scattering experiments, it follows that one can also obtain M_{na} and $\ln f_a$ from light-scattering experiments provided one has done enough experiments to obtain a plot of M_{wa} vs c. Each value of M_{wa} corresponds to one light scattering or one osmotic pressure experiment. So it is evident that one can obtain far more information from a series of sedimentation equilibrium experiments on a few solutions; for instance, five or more different initial concentrations were required to obtain the data shown in Fig. 12 and 13. Since M_{na} can be obtained from osmotic pressure experiments, one can construct a plot of M_{na} vs c if several experiments are performed. With this information M_{wa} and $\ln f_a$ can be obtained since (*90*)

$$\frac{M_1}{M_{wa}} = \frac{d}{dc}\left(\frac{cM_1}{M_{na}}\right) = \frac{M_1}{M_{na}} + c\frac{d}{dc}\left(\frac{M_1}{M_{na}}\right) \tag{132}$$

and because of Eq. (132)

$$\ln f_a = \int_0^c \left(\frac{M_1}{M_{na}} - 1\right)\frac{dc}{c} + \left(\frac{M_1}{M_{na}} - 1\right) \tag{133}$$

It should be apparent that if a physical method gives an average molecular weight or its apparent value at various concentrations for a self-associating solute, then it is potentially possible to analyze the self-association by the methods described here.

It is possible to eliminate the second virial coefficient, BM_1, by various combinations of M_1/M_{na}, M_1/M_{wa}, and $\ln f_a$; the resulting equations are particularly useful for the analysis of monomer–n-mer and indefinite self-associations. Equations (126) and (128) can be combined to give (*34*, *35*)

$$\xi = \frac{2M_1}{M_{na}} - \frac{M_1}{M_{wa}} = \frac{2M_1}{M_{nc}} - \frac{M_1}{M_{wc}} \tag{134}$$

Similarly, Eqs. (126) and (130) can be combined to give

$$\eta = \frac{M_1}{M_{wa}} - \ln f_a = \frac{M_1}{M_{wc}} - \ln f_1 \tag{135}$$

Equations (128) and (130) can be combined to give

$$\nu = \frac{2M_1}{M_{na}} - \ln f_a = \frac{2M_1}{M_{nc}} - \ln f_1 \tag{136}$$

These relations were developed by Chun et al. (*34*). The first two relations are most useful in sedimentation equilibrium experiments (*35*). The third relation is most useful in osmotic pressure experiments. Note that BM_1 has been eliminated in Eqs. (134)–(136), and that the quantities ξ, η, and ν have the same values they would have under ideal conditions.

Analysis of a Monomer-*n*-Mer Association

The association being considered is described by Eq. (114). For this association one notes that the following relations apply (*34*, *35*, *91*):

$$c = c_1 + K_n {c_1}^n \tag{137}$$

$$1 = f_1 + f_n \quad \text{or} \quad f_n = 1 - f_1 \tag{138}$$

$$f_n = K_n {c_1}^n / c = K_n c^{n-1} {f_1}^n \tag{139}$$

The quantities M_1/M_{nc} and M_1/M_{wc} are defined as

$$\frac{M_1}{M_{nc}} = \frac{1}{c}\left(c_1 + \frac{K_n {c_1}^n}{n}\right) = f_1 + \frac{f_n}{n} = \frac{1 + f_1(n-1)}{n} \tag{140}$$

and

$$\frac{M_1}{M_{wc}} = \frac{c}{c_1 + nK_n {c_1}^n} = \frac{1}{n + f_1(1-n)} \tag{141}$$

so that

$$\xi = \frac{2M_1}{M_{nc}} - \frac{M_1}{M_{wc}} = \frac{2 - 2f_1(1-n)}{n} - \frac{1}{n + f_1(1-n)} \tag{142}$$

Equation (142) is quadratic in f_1, hence f_1 is given by

$$f_1 = \frac{n}{4(n-1)^2}\left\{(n-1)\left(\xi + 2 - \frac{2}{n}\right) - \left(\left[(n-1)\left(\xi + 2 - \frac{2}{n}\right)\right]^2 - \left(\frac{8}{n}\right)(n-1)^2(\xi n - 1)\right)^{1/2}\right\} \tag{143}$$

Thus once f_1 is known, it is a simple matter to use Eqs. (138) and (139) to

obtain K_n, since

$$\frac{1 - f_1}{f_1} = K_n(cf_1)^{n-1} \tag{144}$$

A plot of $(1 - f_1)/f_1$ vs $(cf_1)^{n-1}$ has a slope equal to K_n. Once f_1 is known, M_1/M_{wc} is known (see Eq. 141), so that Eq. (126) can be rewritten as

$$\frac{M_1}{M_{wa}} - \frac{1}{n + f_1(1 - n)} = BM_1c \tag{145}$$

A plot of

$$\frac{M_1}{M_{wa}} - \frac{1}{n + f_1(1 - n)} \text{ vs } c$$

has a slope of BM_1. So far it has been assumed n is known. If n is unknown, then one must assume values of n ($n = 2$, 3, etc.) and solve for f_1, K_n, and BM_1 for each choice. The correct choice will give straight line plots which pass through or close to origin. Figure 14 shows an example of a test for

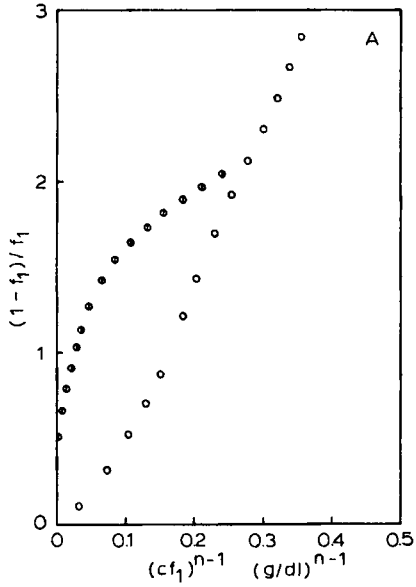

FIG. 14a. Test for a monomer–n-mer self-association using $n = 2$ and $n = 3$. β-Lactoglobulins A and C in 0.2 M glycine buffer (0.1 ionic strength, pH 2.46 at 23.5°C). Results at 11°C with β-lactoglobulin A. $K_2 = 9.58$ dl/g (*35*). Values of f_1 used here were calculated from ξ (see Eq. 142). The plots for $n = 2$ come closest to describing a straight line that passes close to the origin; this indicates the presence of a monomer–dimer association. Attempts to analyze these associations as a monomer–n-mer association with $n > 3$ were unsuccessful.

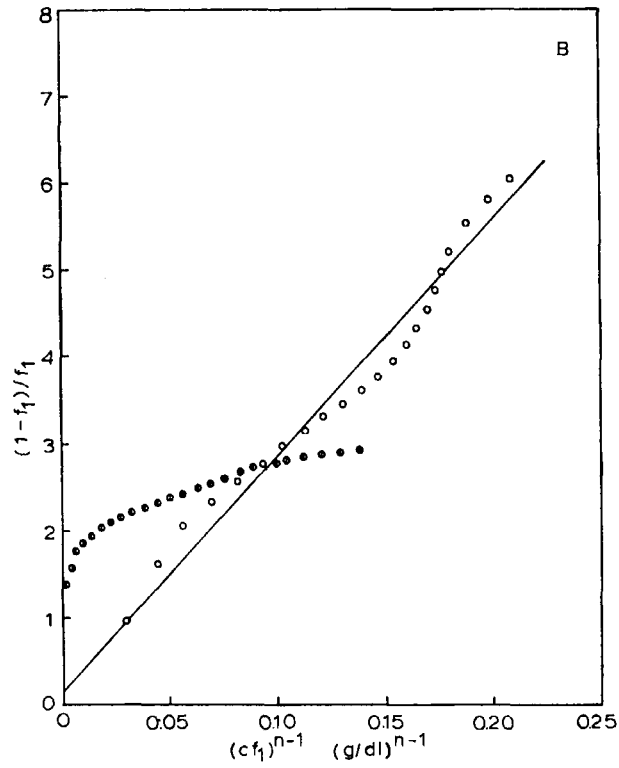

FIG. 14b. Same as Fig. 14a, but these results are at 10°C with β-lactoglobulin C. $K_2 = 27.2$ dl/g (*104*).

a monomer–*n*-mer association; note that the plot for $n = 2$ gives straight lines which come closest to satisfying plots based on Eqs. (144) and (145). It is also possible to use η (see Eq. 135) to try to analyze a monomer–*n*-mer association; for this case

$$\eta = \frac{M_1}{M_{wa}} - \ln f_a = \frac{1}{n + f_1(1 - n)} - \ln f_1 \qquad (146)$$

This equation has one unknown, f_1, which is solved for by successive approximations; remember that $0 < f_1 \leq 1$. A plot based on Eq. (144) using values of f_1 obtained from Eq. (146) is also shown in Fig. 15. For the sedimentation equilibrium experiment it has been shown that the quantity ξ (see Eq. 142) is the least affected by experimental error of the

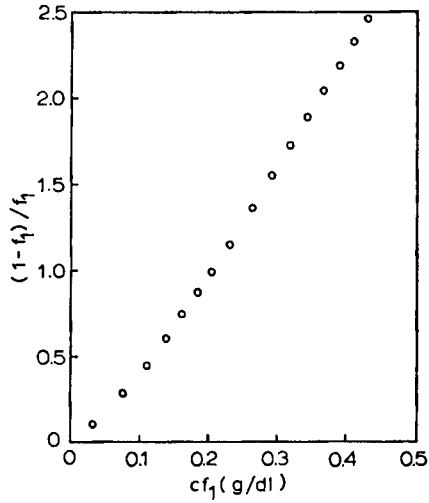

FIG. 15. Self-association of β-lactoglobulin A at 11 °C in 0.2 *M* glycine buffer (ionic strength 0.1, pH 2.46 at 23.5 °C). Test for the presence of a monomer–dimer association using values of f_1 calculated from η (see Eq. 146). From the slope of the best straight line through this plot, a value of $K_2 = 6.56$ dl/g was obtained. Note the difference in this value and the one obtained in Fig. 14a. The plot based on Eq. (142) has been shown to be more reliable (*35*).

three quantities, ξ, η, and ν. On the other hand both ξ and η, being functions of f_1 only, can be used to set up standard plots of ξ vs η for various choices of n. This means experimental values of ξ and η could be calculated, and these calculated values could be compared to a standard table or plot of ξ vs η to see if a monomer–n-mer association is present. Figure 16 shows such a standard plot for a few values of n.

Analysis of Indefinite Self-Associations

A sequential indefinite self-association is described by Eq. (115). Here the association appears to continue without limit. For ideal, dilute solutions or for nonideal solutions for which Eq. (122) applies, one can represent an indefinite self-association as being made up of simultaneous associations of the type (*30*, *32*, *33*, *76*)

$$\begin{aligned} P_1 + P_1 &\rightleftarrows P_2, & K_{12} &= [P_2]/[P_1]^2 \\ P_1 + P_2 &\rightleftarrows P_3, & K_{23} &= [P_3]/[P_1][P_2] \\ P_1 + P_3 &\rightleftarrows P_4, & K_{34} &= [P_4]/[P_1][P_3] \end{aligned} \tag{147}$$

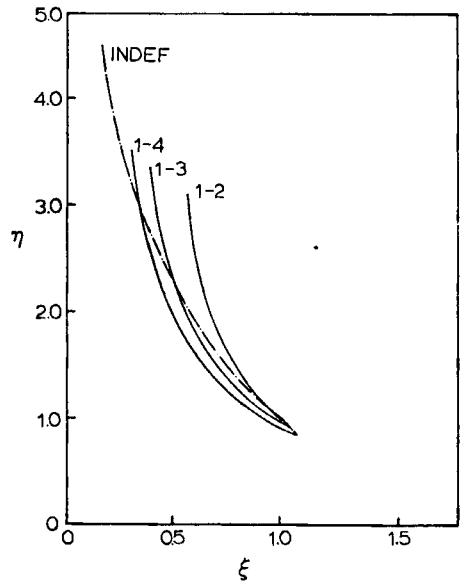

FIG. 16. Standard plots of η (see Eqs. 142 and 161) vs ξ (see Eqs. 146 and 162) for a monomer–dimer (1–2), a monomer-trimer (1–3), a monomer-tetramer (1–4), and a sequential, indefinite (INDEF) self-association. For these associations η and ξ are each functions of f_1 ($0 \leq f_1 \leq 1$); thus, for each model, one can assume values of f_1 and construct standard curves which can be used to test for the type of self-association that might be present (*34*).

and so on. Here $[P_i]$ represents the molar concentration of species i ($i = 1, 2, \ldots$), and K_{ij} represents the molar equilibrium constant. The Eqs. (147) can be rearranged to give

$$\begin{aligned} [P_2] &= K_{12}[P_1]^2 \\ [P_3] &= K_{12}K_{23}[P_1]^3 \\ [P_4] &= K_{12}K_{23}K_{34}[P_1]^4 \end{aligned} \tag{148}$$

and so on. In order to analyze an indefinite self-association, one must make some assumptions regarding the molar equilibrium constants, the K_{ij}; otherwise, the analysis becomes formidable. For a sequential indefinite self-association (an association in which all species appear to be present), one can assume that all molar equilibrium constants are equal, i.e., assume

$$K_{12} = K_{23} = K_{24} = \cdots = K \tag{149}$$

Now convert concentrations to the gram/milliliter scale, C_i; thus we obtain

$$C_2 = 2\left(\frac{1000K}{M_1}\right)C_1^2 = 2kC_1^2$$
$$C_3 = 3\left(\frac{1000K}{M_1}\right)^2 C_1^3 = 3k^2C_1^3 \tag{150}$$

and so on. The total concentration of the associating solute becomes

$$\begin{aligned} C &= C_1 + 2kC_1^2 + 3k^2C_1^3 + 4k^3C_1^4 + \cdots \\ &= C_1(1 + 2kC_1 + 3k^2C_1^2 + 4k^3C_1^3 + \cdots) \\ &= C_1/(1 - kC_1)^2, \qquad \text{if } kC_1 < 1 \end{aligned} \tag{151}$$

Under these circumstances Eq. (119) becomes

$$\ln y_i = i\hat{B}M_1C = iBM_1c \tag{119a}$$

Since $C = c/1000$, then $\hat{B}M_1 = 1000BM_1$. Note that M_1/M_{wa} can be written as

$$\frac{M_1}{M_{wa}} = \frac{M_1}{M_{wc}} + \hat{B}M_1C \tag{152}$$

Now M_1/M_{wa} is the same whether the gram/liter or the gram/milliliter concentration scale is used; this follows from Eq. (123) since $d \ln c = d \ln C$. Thus it follows that

$$\hat{B}M_1C = BM_1c \tag{153}$$

The number-average molecular weight, M_{nc}, is defined as

$$M_n = \sum_i n_iM_i/\sum_i n_i = w/\sum_i w_i/M_i$$

This definition can be recast as

$$M_{nc} = C/\sum_i (C_i/M_i)$$

It follows that

$$\frac{C}{M_{nc}} = \sum_i \frac{C_i}{M_i}$$

For a self-associating system $M_2 = 2M_1$, $M_3 = 3M_1$, etc., so that

$$\begin{aligned} \frac{CM_1}{M_{nc}} &= M_1 \sum_i \frac{C_i}{M_i} = \sum_i \frac{C_i}{i} \\ &= C_1 + kC_1^2 + k^2C_1^3 + k^3C_1^4 + \cdots \\ &= C_1/(1 - kC_1), \qquad \text{if } kC_1 < 1 \end{aligned} \tag{154}$$

Division of Eq. (154) by Eq. (151) leads to

$$M_1/M_{nc} = 1 - kC_1 \tag{155}$$

Similarly it can be shown that

$$\frac{M_1}{M_{wc}} = \frac{1 - kC_1}{1 + kC_1} \tag{156}$$

The expressions for M_1/M_{nc} and for M_1/M_{wc} are formally the same as those obtained by Flory (*92*) for linear condensation polymerization. Flory obtained $M_0/M_n = 1 - p$ and $M_0/M_w = (1 - p)/(1 + p)$; here M_0 is the molecular weight of the repeating unit and $p(0 \leq p \leq 1)$ is the extent of polymerization.

Equation (151) can be rearranged to give

$$C_1/C = f_1 = (1 - kC_1)^2 \tag{157}$$

from which it follows that

$$\sqrt{f_1} = 1 - kC_1 = 1 - kCf_1 \tag{158}$$

or

$$(1 - \sqrt{f_1})/f_1 = kC \tag{158a}$$

Once $\sqrt{f_1}$ or f_1 has been obtained, one can use Eq. (158a) to obtain k, since a plot of $(1 - \sqrt{f_1})/f_1$ vs C would be a straight line passing through the origin and having a slope of k. Equation (158) could also be used for this purpose. Experimental error may cause the plot not to go through the origin, but the plot should come close to it. We can use Eqs. (152), (156), and (158) to show that

$$\begin{aligned} \frac{M_1}{M_{wa}} &= \frac{1 - kC_1}{1 + kC_1} + \hat{B}M_1C \\ &= \frac{\sqrt{f_1}}{2 - \sqrt{f_1}} + \hat{B}M_1C \end{aligned} \tag{159}$$

Similarly, M_1/M_{na} can be expressed as

$$\begin{aligned} \frac{M_1}{M_{na}} &= 1 - kC_1 + \frac{\hat{B}M_1C}{2} \\ &= \sqrt{f_1} + \frac{\hat{B}M_1C}{2} \end{aligned} \tag{160}$$

For an indefinite self-association the quantities ξ and η (see Eqs. 134 and

135) are given by

$$\xi = 2\sqrt{f_1} - \frac{\sqrt{f_1}}{2 - \sqrt{f_1}} \tag{161}$$

and

$$\eta = \frac{\sqrt{f_1}}{2 - \sqrt{f_1}} - \ln f_1 \tag{162}$$

Equation (161) is quadratic in $\sqrt{f_1}$, and $\sqrt{f_1}$ is obtained from

$$\sqrt{f_1} = (1/4)\{(\xi + 3) - \sqrt{(\xi + 3)^2 - 16\xi}\} \tag{163}$$

One obtains f_1 or $\sqrt{f_1}$ in Eq. (162) by successive approximations. Once f_1 or $\sqrt{f_1}$ is known, k can be obtained from plots based on Eq. (158) or (158a). The second virial coefficient $\hat{B}M_1$ is obtained from Eq. (161) since

$$\frac{M_1}{M_{wa}} - \frac{\sqrt{f_1}}{2 - \sqrt{f_1}} = \hat{B}M_1C \tag{164}$$

A plot of

$$\left\{\frac{M_1}{M_{wa}} - \frac{\sqrt{f_1}}{2 - \sqrt{f_1}}\right\}$$

vs C will have a slope of $\hat{B}M_1$. This plot should go through the origin, but experimental error may cause it to miss the origin slightly. Figure 17 shows plots based on Eqs. (158a) and (160).

The indefinite self-association considered above is one for which all molar equilibrium constants are equal, and it also implies that the standard Gibbs free energy for the addition of monomer (or unimer) to an aggregate of any size, including monomer, is the same. Now suppose that only the standard Gibbs free energy for the dimerization is different from the standard Gibbs free energy for formation of higher aggregates. This would mean that in Eqs. (147) and (148), $K_{12} \neq K_{23}$, K_{34}, etc., but that $K_{23} = K_{34} = \cdots = K$. In this case it can be shown that (*93*)

$$C = C_1\left[1 + \frac{k_{12}C_1(2 - kC_1)}{(1 - kC_1)^2}\right] \tag{165}$$

if $kC_1 < 1$. Here

$$k_{12} = 1000K_{12}/M_1 \tag{166}$$

and

$$k = 1000K/M_1 \tag{167}$$

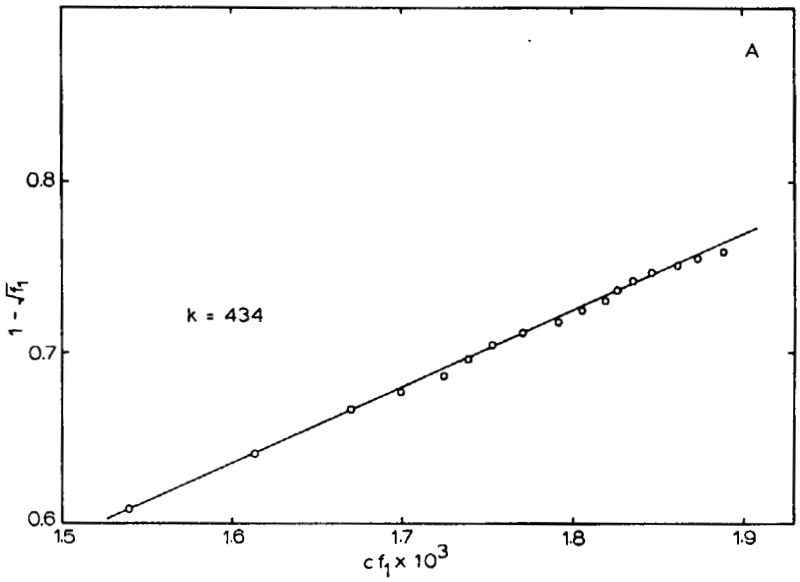

FIG. 17a. Test for a sequential, indefinite self-association. Self-association of β-lactoglobulin A at 16°C in 0.2 *M* acetate buffer (ionic strength 0.1, pH 4.61 at 22.5°C). Using the data of Adams and Lewis (*32*), f_1 was calculated from ξ (see Eq. 161) and used for the evaluation of k and $\hat{B}M_1$. Evaluation of k from a plot based on Eq. (158). By another method Adams and Lewis obtained $k = 400$ ml/g and $\hat{B}M_1 = 1.6$ ml/g. Note the amazing effect of the solution conditions (see Fig. 14) on the self-association of the β-lactoglobulin A.

Similarly, it can be shown that

$$\frac{M_1}{M_{wc}} = \frac{\left[1 + \dfrac{k_{12}C_1(2 - kC_1)}{(1 - kC_1)^2}\right]}{\left[1 + \dfrac{k_{12}C_1(4 - 3kC_1 + k^2C_1^2)}{(1 - kC_1)^3}\right]} \tag{168}$$

and that

$$\frac{M_1}{M_{nc}} = \frac{\left[1 + \dfrac{k_{12}C_1}{(1 - kC_1)}\right]}{\left[1 + \dfrac{k_{12}C_1(2 - kC_1)}{(1 - kC_1)^2}\right]} \tag{169}$$

The quantity ξ (see Eqs. 134 and 135) would involve two unknowns, $x = k_{12}C$ and $y = kC_1$, and it would be awkward to solve for these

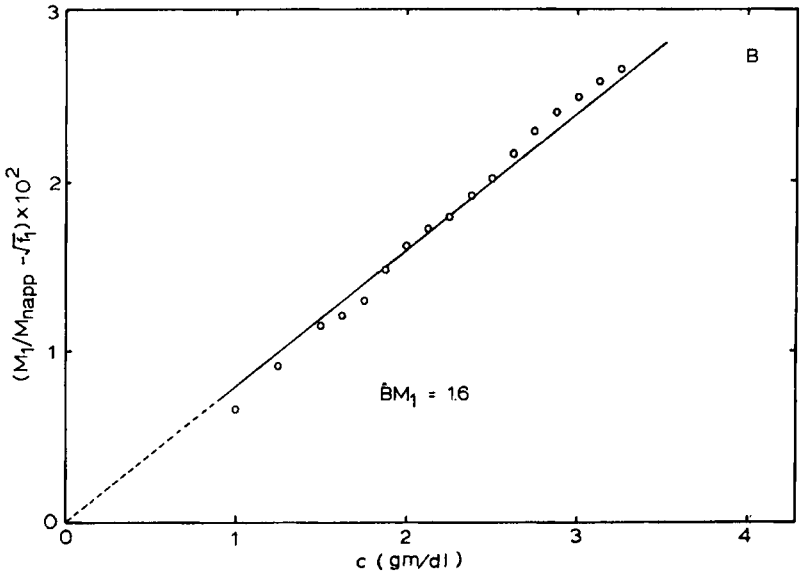

FIG. 17b. Evaluation of $\hat{B}M_1$ from a plot based on Eq. (160). See the legend of Fig. 17a.

unknowns. One would have to try to evaluate x and y at concentration c by Monte Carlo methods or by other numerical methods (*94*). It appears one can actually use Eqs. (165), (168), and (169) to obtain one equation in one unknown ($\hat{B}M_1$), but the procedure for doing it is complicated and must be tested thoroughly.

Other Types of Indefinite Self-Associations

Suppose no trimer, pentamer, heptamer, etc. were present. Two types of self-associations arise: one in which all molar equilibrium constants are equal, and one for which K_{12} differs from all other molar equilibrium constants. If all molar equilibrium constants are equal then one obtains (*93*)

$$\begin{aligned} C &= C_1 + 2kC_1^2 + 4k^3C_1^4 + 6k^5C_1^6 + \cdots \\ &= C_1[1 + 2kC_1\{1 + 2k^2C_1^2 + 3k^4C_1^4 + \cdots\}] \\ &= C_1\left[1 + \frac{2kC_1}{(1 - k^2C_1^2)^2}\right], \qquad \text{if } kC_1 < 1 \end{aligned} \tag{170}$$

Similarly, one notes that ξ (see Eq. 134) becomes

$$\xi = \frac{2\left[1 + \frac{kC_1}{(1 - k^2C_1^2)}\right]}{\left[1 + \frac{2kC_1}{(1 - k^2C_1^2)^2}\right]} - \frac{\left[1 + \frac{2kC_1}{(1 - k^2C_1^2)^2}\right]}{\left[1 + \frac{4kC_1(1 + k^2C_1^2)}{(1 - k^2C_1^2)^3}\right]} \tag{171}$$

This equation has only one unknown, kC_1. Since $0 \leq kC_1 \leq 1$, one solves for kC_1 by successive approximations. Once kC_1 is known, it is an easy matter to obtain C_1 from Eq. (170). Now let $X = kC_1$; a plot of X vs C_1 will have a slope of k. Here $k = (1000K/M_1)$ is the intrinsic equilibrium constant.

Now suppose that $K_{12} \neq K_{24}$, K_{26}, etc., but that $K_{24} = K_{26} = \cdots = K$. Letting $k_{12} = 1000K_{12}/M_1$ and $k = 1000K/M_1$, the expression for the total concentration of the associating solute is *(95)*

$$\begin{aligned} C &= C_1\left[1 + \frac{2k_{12}C_1}{(1 - kk_{12}C_1^2)^2}\right] \\ &= C_1\left[1 + \frac{2x}{(1 - xy)^2}\right] \end{aligned} \tag{172}$$

Here $y = kC_1$ and $x = k_{12}C_1$. Note that $0 \leq x \leq 1$ and $0 \leq y \leq 1$. For this association the expressions for M_1/M_{nc} and M_1/M_{wc} become

$$\frac{M_1}{M_{nc}} = \frac{\left[1 + \frac{x}{(1 - xy)}\right]}{\left[1 + \frac{2x}{(1 - xy)^2}\right]} \tag{173}$$

and

$$\frac{M_1}{M_{wc}} = \frac{\left[1 + \frac{2x}{(1 - xy)^2}\right]}{\left[1 + \frac{4x(1 + xy)}{(1 - xy)^3}\right]} \tag{174}$$

The expression for ξ (see Eq. 134) would have two unknowns x and y, which would have to be solved at every point (at every value of ξ that was used). We would have to use methods similar to those used with the sequential indefinite self-association for which $k_{12} \neq k$. Some recent developments in our laboratory indicate that we can use Eqs. (172) and (173) to obtain an equation in one unknown, $\hat{B}M_1$. We are currently evaluating and testing this idea.

Indefinite self-associations may be important in the self-assembly of virus coat protein subunits. One could have a linear or helical association of subunits, and equations that are similar to those used here have been developed for these situations. For more details the reader should consult the papers by Chun (*96*). Pekar and Frank (*97*) have studied the self-association of insulin near neutral pH; at pH 7.4 they believe that the self-association can be described by

$$nP_1 \rightleftarrows qP_2 + hP_6 + jP_{12} + mP_{18} + \cdots \tag{175}$$

In other words, the higher aggregates are multiples of the hexamer. For bovine insulin A the monomer molecular weight is $M_1 = 5733$ (*98*).

The Monomer-Dimer-Trimer and Related Self-Associations

A monomer–dimer–trimer association is described by (*29, 30*)

$$nP_1 \rightleftarrows qP_2 + mP_3 \tag{176}$$

When Eq. (119) applies, the following relations obtain.

$$c = c_1 + K_2 c_1^{\,2} + K_3 c_1^{\,3} \tag{177}$$

$$\frac{cM_1}{M_{na}} = c_1 + \frac{K_2 c_1^{\,2}}{2} + \frac{K_3 c_1^{\,3}}{3} + \frac{BM_1 c^2}{2} \tag{178}$$

$$\frac{1}{\dfrac{M_1}{cM_{wa}} - BM_1} = \frac{cM_{wc}}{M_1} = c_1 + 2K_2 c_1^{\,2} + 3K_3 c_1^{\,3} \tag{179}$$

and

$$\ln f_a = \ln f_1 + BM_1 c \tag{180}$$

or

$$\alpha = cf_a = c_1 \exp(BM_1 c) \tag{181}$$

We can combine Eqs. (177–179) and (181) to obtain (*29, 30*)

$$\begin{aligned} \frac{6cM_1}{M_{na}} - 5c &= 2c_1 + 3BM_1 c^2 - \frac{1}{\dfrac{M_1}{cM_{wa}} - BM_1} \\ &= 2\alpha \exp(-BM_1 c) + 3BM_1 c^2 - \frac{1}{\dfrac{M_1}{cM_{wa}} - BM_1} \end{aligned} \tag{182}$$

This equation contains only one unknown, BM_1, which can be solved for by successive approximations. Alternatively Eq. (182) can be recast as

$$\frac{6M_1}{M_{na}} - 5 = 2f_a \exp(-BM_1 c) + 3BM_1 c - \frac{1}{\frac{M_1}{M_{wa}} - BM_1 c} \tag{183}$$

The only unknown here is BM_1. This can be solved for by successive approximation. Instead of solving Eq. (182) or (183) point by point, one could set up an array of equations from several (20 to 30 or more) data points, and use a Monte Carlo procedure to find the best BM_1 as measured by the sum of the square of the error or by the sum of the absolute value of the error (*99*). Here the error ε would be defined as

$$\frac{\Delta\left(\frac{6M_1}{M_{na}} - 5\right)}{\left(\frac{6M_1}{M_{na}} - 5\right)_{\text{obs}}} = \varepsilon \tag{184}$$

and

$$\Delta\left(\frac{6M_1}{M_{na}} - 5\right) = \left(\frac{6M_1}{M_{na}} - 5\right)_{\text{calc}} - \left(\frac{6M_1}{M_{na}} - 5\right)_{\text{obs}} \tag{184a}$$

Sometimes with very strong self-associations, the plot of $[(M_1/M_{wa}) - 1]/c$ vs c, which is required for the evaluation of $\ln f_a$ (see Eq. 129), may be quite steep in the low concentration region. Figure 18 shows such a plot for a simulated monomer–dimer–trimer association; the intercept at $c = 0$ is $-K_2 + BM_1$. The greatest contribution to the integral required for $\ln f_a$,

$$\ln f_a = \int_0^c \left(\frac{M_1}{M_{wa}} - 1\right)\frac{dc}{c}$$

comes from the region of lowest solute concentration. This is the area where the experimental error may be the worst; and this may cause problems in the application of Eqs. (183) and (184). One way to avoid this is to calculate $\ln f_a/f_{a^*}$, where

$$\ln f_a/f_{a^*} = \int_{c^*}^c \left(\frac{M_1}{M_{wa}} - 1\right)\frac{dc}{c} \tag{185}$$

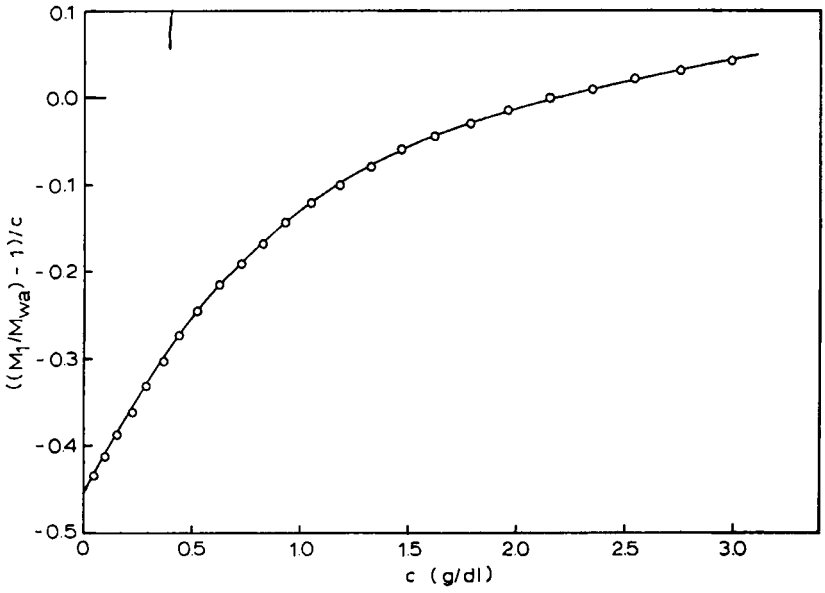

FIG. 18. Plot required for the evaluation of $\ln f_a$ (see Eq. 129). Here a simulated monomer–dimer–trimer association was used; $K_2 = 0.65$ dl/g, $K_3 = 0.5$ dl/g, and $BM_1 = 0.2$ dl/g. The intercept of this plot is $-K_2 + BM_1 = -0.45$. The actual shape of this curve depends on the values of the K_i and the BM_1; with stronger self-associations this plot becomes much steeper in the vicinity of $c = 0$.

Here c^* is a low concentration; the choice is arbitrary. What we want to do is get rid of the troublesome part of the $[(M_1/M_{wa}) - 1]/c$ vs c plot. We can then recast Eq. (183) as

$$\frac{f_1}{f_{1^*}} = \frac{\left[\dfrac{6M_1}{M_{na}} - 5 + 3BM_1c - \dfrac{1}{\dfrac{M_1}{M_{wa}} - BM_1c}\right]}{\left[\dfrac{6M_1}{M_{na^*}} - 5 + 3BM_1c^* - \dfrac{1}{\dfrac{M_1}{M_{wa^*}} - BM_1c^*}\right]} \tag{186}$$

Multiplication of both sides of this equation by $\exp[BM_1(c - c^*)]$ leads

to (99)

$$\frac{f_a}{f_{a^*}} = \frac{f_1}{f_{1^*}} \exp[BM_1(c - c^*)]$$
$$= \frac{\left[\dfrac{6M_1}{M_{na}} - 5 + 3BM_1c - \dfrac{1}{\dfrac{M_1}{M_{wa}} - BM_1c}\right] \exp[BM_1(c - c^*)}{\left[\dfrac{6M_1}{M_{na^*}} - 5 + 3BM_1c^* - \dfrac{1}{\dfrac{M_1}{M_{wa^*}} - BM_1c^*}\right]} \quad (187)$$

Here one can set up an array of data points and use a Monte Carlo procedure to find the best value of BM_1 to fit the array. We did this with the self-association of adenosine-5′-triphosphate (ATP) in isotonic saline, and showed that a monomer–dimer–trimer self-association gave the best description of the observed self-association. Figure 19 shows a plot of

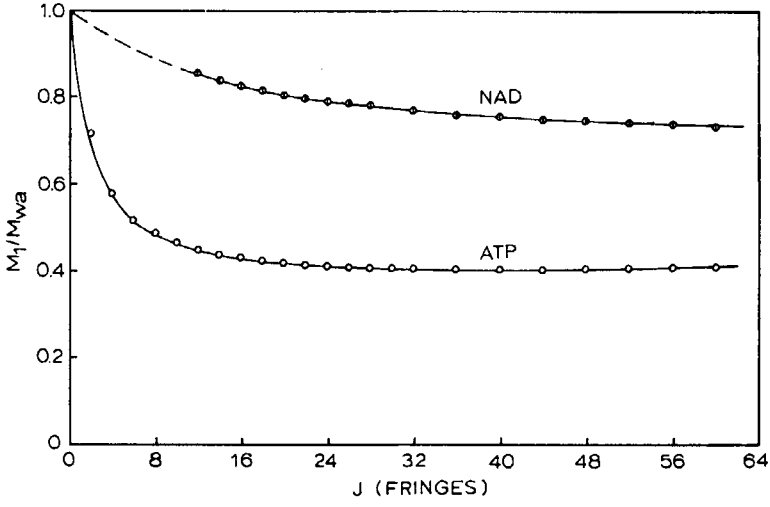

FIG. 19. Self-association of small, ionizable molecules. These plots of M_1/M_{wa} vs J give a comparison of the self-association of two nucleotides, Adenosine-5′-triphosphate (ATP) and Nicotine adenine dinucleotide (NAD), in isotonic saline at 20°C. These solutions were dialyzed in a hollow fiber dialyzer with a 200 Dalton cutoff. It is evident that ATP associates more strongly than the NAD. ATP undergoes a monomer-dimer-trimer association (*99*). Experiments are still underway with NAD; preliminary results suggest a sequential, indefinite self-association may be present.

M_1/M_{wa} vs c at 10°C for ATP in isotonic saline; on the same plot we have also shown some preliminary results with the self-association of NAD (nicotine adenine dinucleotide) in isotonic saline. The self-association for ATP (*99*) is stronger than that for NAD (*100*), purine and cytidine (*33*, *73*), or that observed with various nucleosides (*74*, *75*).

Equations analogous to Eq. (182) or (183) can be developed for other related self-associations, such as a monomer–dimer–tetramer. For this association, the analog of Eq. (183) is

$$\frac{8M_1}{M_{na}} - 6 = 3c_1 + 4BM_1c - \frac{1}{\dfrac{M_1}{M_{wa}} - BM_1c} \tag{188}$$

Other Self-Associations

Teller (*101*) has considered the case of discrete self-associations in which the equilibrium constants are equal. Šolc and Elias (*85*) have given a very detailed treatment of a self-association involving a heterogeneous unimer (monomer). The discussion in this paper so far has been restricted to self-associations involving a homogeneous unimer (or monomer). Šolc and Elias (*85*) have given a very elegant treatment of a more complicated case. Their paper is the opening wedge in a vast area.

Factors Influencing Self-Associations

With a self-associating solute one can only add the solute itself to the solution; the subsequent self-association equilibrium that sets in depends on various factors such as temperature, pH, ionic strength, and the presence or absence of other additives or ions. Various types of chemical interactions may be involved. For example, with soaps and detergents in aqueous solution, hydrophobic interactions are involved. These associations can be influenced by the position of the polar group for polar detergents as well as by the ionic strength of the medium (*69–72*). With purine, cytidine, and various nucleosides, it is believed that base stacking is an important factor (*33*, *73–75*). Ts'o (*75*) was able to prepare a chemically modified nucleoside in which no hydrogen bonds could be formed, yet it associated very strongly in aqueous solution. This association was attributed to base stacking (*75*). Recently we have done some studies on the temperature-dependent self-association of the disodium salt of adenosine-5′-triphosphate (ATP) dissolved in and dialyzed against isotonic

saline (0.154 *M* NaCl); the availability of a hollow fiber dialyzer with a low molecular weight cutoff made these studies possible (*99*). Our results indicated that ATP underwent a monomer–dimer–trimer self-association; the association was greater at lower temperatures. Furthermore the molar association equilibrium constant for the dimerization was greater than that observed by others for purine, cytidine, or various nucleosides. One would think that the triphosphate group, since it ionizes, would inhibit self-association; yet our results indicated a much stronger self-association.

With proteins metal ions are sometimes involved. Kakiuchi (*102*) showed that Zn^{2+} is needed for the self-association of an anylase obtained from *B. subtilis*. Electrostatic repulsions and attractions are involved in the self-association of the β-lactoglobulins at low pH (pH 2 to 3). An increase of salt increases the degree of aggregation; Types A, B, and C show a monomer–dimer association under these conditions (*31*, *35*, *91*, *103–105*). In the pH range 4 to 5.7 the association behavior is quite different. β-Lactoglobulin A shows a very strong, temperature-dependent self-association which has been characterized as an indefinite (*32*, *93*) or as a dimer–octamer (*105*, *106*). Sedimentation equilibrium experiments on three different batches of β-lactoglobulin A in acetate buffer at pH 4.7 and ionic strengths varying from 0.1 to 0.16 have shown that the 18,422 Dalton monomer unit is present and would be the limiting species in the vicinity of zero protein concentration. Experiments carried out using a photoelectric scanner have indicated apparent weight average (M_{wa}) molecular weights as low as 21,000 at very low concentrations, and the trend of these M_{wa} would go to the 18,422 unit. The genetic variants β-lactoglobulins B and C do not associate as strongly. McKenzie (*107*) maintains that —COOH groups are involved in the strong self-associations of β-lactoglobulin A in the pH range 4 to 5.7; he diminished the self-association by chemically modifying the —COOH group. The self-association of three genetic variants of α_{s_1}-casein were studied by Schmidt (*108*); two of the variants showed similar behavior, whereas the other one differed. The effect of various ions, presumably by ion binding, on the self-association of apoferritin has been shown by light-scattering experiments carried out on the apoferritin in different buffer solutions (*109*). Chymotrypsinogen associates only at low ionic strengths (*110*, *111*) whereas chymotrypsin associates at higher ionic strength (*80*). The addition of diisopropyl fluorophosphate (DIP) to chymotrypsin stops the enzymatic activity, but it does not stop the self-association (*38*). Eisenberg and his associates (*112*, *113*) have shown that bovine lactate dehydrogenase associates; Chun et al.

(*114*) have shown that this association is a sequential indefinite self-association. It was shown by Eisenberg and his associates (*113*) that a small amount of diethyl stilbesterol inhibited the self-association; this indicates the presence of hydrophobic bonds. Furthermore they were able to cross-link the associating species and still show some biological activity which indicated that the association and active sites were in different locations.

Clearly from this discussion it is apparent that various forces are involved in self-association, and that genetic variation can also influence the self-association. A very interesting discussion about the forces involved in protein associations and methods to test for them is given in the paper by Timasheff (*115*).

Other Methods for Studying Self-Associations

Equilibrium Thermodynamic Methods

Since M_{na} and M_{wa} are interrelated for self-associating solutes, one can use any technique that will give values of M_{wa} or M_{na} and perform a series of experiments with several solutions of different concentrations. Then plots of M_{na} or M_{wa} vs c or M_1/M_{na} or M_1/M_{wa} vs c can be constructed, and the analysis can be done in the same way that has been described here. For instance, M_1/M_{wa} is obtained from plots of M_1/M_{na} vs c since (see Eq. 132) (*90*)

$$\frac{M_1}{M_{wa}} = \frac{d}{dc}\left(\frac{cM_1}{M_{na}}\right) = \frac{M_1}{M_{na}} + c\frac{d}{dc}(M_1/M_{na}) \tag{132}$$

Similarly one notes that (*90*)

$$\ln f_a = \int_0^c \left(\frac{M_1}{M_{na}} - 1\right)\frac{dc}{c} + \left(\frac{M_1}{M_{na}} - 1\right) \tag{133}$$

The big disadvantage here is that each point on the plots of M_{wa} or M_{na} vs c corresponds to one solution, so a large amount of material is required. On the other hand one can cover the same range of M_{na} or M_{wa} vs c in sedimentation equilibrium experiments with only a few (four or more) solutions of different initial concentrations.

Two techniques that give M_{wa} are elastic light scattering and low-angle X-ray scattering. Extensive studies on the self-association of the β-lactoglobulins A and B, using light scattering, have been reported by Timasheff and Townend and their associates (*103, 106*). At low pH (pH 2 to 3.5) the

β-lactoglobulins A and B undergo a monomer–dimer association. These associations have also been studied by sedimentation equilibrium experiments, and good agreement has been found between the two techniques (*35*, *91*). M_{na} can be obtained from high-speed membrane osmometry or vapor pressure osmometry. The monomer–dimer self-association of soybean proteinase inhibitor was studied by Harry and Steiner (*116*) using high-speed membrane osmometry. The self-association of purine in aqueous solutions has been examined by vapor pressure osmometry (*75*, *117*) and by sedimentation equilibrium (*33*, *73*). Excellent agreement has been obtained by the two methods; both methods indicated the presence of a sequential indefinite self-association. This association is attributed to base stacking. Elias (*72*) has followed the self-association of some nonionic detergents by light-scattering, vapor pressure osmometry, and sedimentation equilibrium experiments; the degree of aggregation and the equilibrium constants obtained by the three methods agreed remarkably well.

Transport Methods

Gilbert and his associates (*118–121*) have proposed a method for analyzing self-associations from the shape of the moving boundary in a sedimentation velocity experiment. In order to solve the continuity equation when self-associations occur, Gilbert (*118*) was forced to make four assumptions: (a) The centrifugal field is constant, (b) the cell has a constant cross-sectional area, (c) there is no diffusion in a moving boundary, and (d) the velocity of the *n*-mer relative to the monomer is constant. For the sedimentation velocity experiment the first three assumptions are false; only the last assumption may be true. The neglect of diffusion was necessary so that the continuity equation could be solved. Only recently with very sophisticated computational procedures has it been possible to include diffusion in the continuity equation for self-associations (*122*, *123*) or mixed associations (*124*, *125*). Nevertheless, Gilbert's methods did stir up quite a bit of interest in the study of self-associations. His theory indicated the moving boundary should be bimodal for a monomer–*n*-mer association when $n \geq 3$. However, it has been shown by Fujita (*126*) that one may still encounter unimodal boundaries for a monomer–trimer association under some conditions. Cox, who has done some elegant computer simulation studies on self-associations, has shown that unimodal boundaries can be encountered with monomer–trimer and monomer–tetramer associations (*122*, *123*). For a monomer–trimer association which has $M_1 \leq 50{,}000$ Daltons, he has shown that diffusion can mask

the bimodality; the same thing can happen in a monomer–tetramer association if $M_1 \leq 20{,}000$. It has been pointed out that the presence of dimer in these associations could cause unimodal peaks (*122*, *123*). The Gilbert method may fail when intermediate species coexist in rapid equilibrium with a monomer and its highest n-mer (*127*). Although the molecular weights of the associating species have the same relation $M_j = jM_1$ ($j = 2, 3, \ldots$), there is no known relation between sedimentation coefficients of the associating species. If we knew the shape of the species we might be able to predict the relation between the sedimentation coefficients of the associating species. Finally, at present no plots comparable to those based on Eqs. (134)–(136) are available for sedimentation velocity experiments; clearly, the sedimentation equilibrium method does have an advantage.

The Gilbert method has also been applied to moving boundary electrophoresis (*128*). The application of the Gilbert method to various transport methods has been discussed by Cann (*125*) and also by Nichol, Bethune, Kegeles, and Hess (*128*). Winzor and Scheraga (*38*) have tested the Gilbert method using gel filtration chromatography. They have shown that derivatives of the elution profiles resemble the schlieren patterns obtained by electrophoresis or sedimentation velocity. In fact, they claim and do demonstrate a difference in the derivatives of the elution profiles between self-associating and noninteracting proteins. From these elution profiles they can calculate the elution volume, V_e, which for self-associations exhibits a concentration dependence similar to that exhibited by sedimentation coefficients of self-associating solutes. With self-associations they measure an apparent weight-average elution volume, $V_{ew\ app}$. The concentration dependence of the elution volume is quite different for noninteracting and for self-associating systems. In fact a plot of $V_{ew\ app}$ vs c resembles a plot of $1/s_{wa}$ vs c; here s_{wa} is the apparent weight-average sedimentation coefficient. The elution volume, V_e, is proportional to molecular weight for a series of polymers (*129*), and this fact can be used to estimate molecular weights from gel filtration chromatography. This method has the advantage of speed and simplicity; and it has also been applied to a study of the mixed association between lysozyme and ovalbumin (*130*). More details about this technique will be found in the monograph by Winzor and Nichol (*37*).

A very beautiful and elegant method for studying chromatography directly on a column, and especially the chromatographic behavior of chemically reacting systems, is the scanning method developed by Brumbaugh and Ackers (*130*, *131*). Quartz columns packed with sephadex are

used. A high intensity lamp is placed on one side of the column and a photomultiplier is placed on the other side; the output from the photomultiplier is fed to a computer. A motor is used to move the column up or down so that various levels can be scanned. Even though light scattering causes a high background absorbance with only buffer and the sephadex gel, Brumbaugh and Ackers (*130, 131*) were able to show a linear relation between protein concentration and absorbance in the absorbance range of 2 to 3. With these experiments the weight-average partition coefficients, σ_w, between the gel phase and the liquid phase can be measured. The weight-average elution volume, V_{ew}, can also be obtained. An empirical relation between partition coefficients and molecular weights has been established (*131*). For self-associations both σ_w and V_{ew} are functions of the total concentration of the associating solute, and they can be used to estimate the equilibrium constant (*3*). Henn and Ackers (*132*) have done very elegant studies of the monomer–dimer self-association of D-amino acid oxidase apoenzyme; this association was studied at several temperatures. The van't Hoff plot of ln K_2 vs $1/T$ gave a reversed S-shape curve. This was interpreted to mean that a conformational equilibrium accompanied the self-association. With the aid of other physical methods, optical rotatory dispersion and concentration difference spectra in the UV region, they were able to calculate the conformational equilibrium constant.

Chun et al. (*114*) have shown that one can obtain the weight fraction of monomer, f_1, from values of the weight-average partition coefficients, σ_n, when self-associations are present. They have developed equations applicable to various types of self-associations. The σ_w could also be related empirically to molecular size. Chun et al. (*114*) have shown that the self-association of bovine liver L-glutamate dehydrogenase reported by Eisenberg and Tompkins (*112*) was a sequential indefinite self-association. Chun et al. (*114*) also studied this self-association by analytical gel chromatography; their plot of σ_w vs c agreed with the plot predicted for a linear indefinite self-association.

Godschalk (*133*) has developed a very sophisticated, computational method for determining the translational diffusion coefficients of self-associating species. The method works best with materials having an absorption spectrum in the range of 220 to 560 nm, so that a photoelectric scanner equipped with a data acquisition system can be used to reduce the tediousness of the calculations. With this method it is possible to evaluate diffusion coefficients and also to enumerate the number of associating species, if this is not known a priori.

In the discussion of the other methods for studying self-associations, we have not considered what would happen if both thermodynamic (equilibrium) and transport experiments on the same associating solute were carried out under identical solution conditions. Would it be possible to evaluate additional information about the associating solute, such as the sedimentation coefficients of the associating species? Such experiments have been performed. Kakiuchi and Williams (*134*) have studied the self-association of a γ-G globulin from multiple myeloma; the solvent was 8 *M* urea, buffered at pH 7.

If we assume that interacting flows are absent in a multicomponent system, then we can combine the two techniques. This is an assumption that one is forced to make at present. The apparent weight-average sedimentation coefficient, s_{wa}, is defined by (*42*)

$$s_{wa} = \frac{s_{wc}}{1 + gc} \qquad \text{(Model I)} \tag{189}$$

or by a second model (*42*)

$$\frac{1}{s_{wa}} = \frac{1}{s_{wc}} + gc \qquad \text{(Model II)} \tag{190}$$

Here s_{wc}, the weight-average sedimentation coefficient, is defined by

$$s_{wc} = \frac{\sum c_i s_i}{c} \tag{191}$$

For a monomer–dimer association

$$s_{wc} = \frac{s_1 + K_2 c_1 s_2}{1 + K_2 c_1} \tag{192}$$

The quantity g or $\boldsymbol{g}$ is the hydrodynamic concentration dependence parameter associated with ordinary sedimentation coefficient measurements on nonassociating solutes. Note that s_1 is the sedimentation coefficient of the monomer at infinite dilution, and s_2 is the sedimentation coefficient of the dimer. Thus

$$\lim_{c \to 0} s_{wa} = s_1 \tag{193}$$

or

$$\lim_{c \to 0} 1/s_{wa} = 1/s_1 \tag{193a}$$

For very strong self-associations it may be difficult to obtain s_1 from the

limiting slope of a plot of s_{wa} or $1/s_{wa}$ vs c; thus one may have to estimate s_1 from experiments conducted under nonassociating conditions. It will have to be assumed that s_1 does not change with the different solution conditions. Kakiuchi and Williams (*111*, *134*) pointed out that Eq. (189) became linear at high solute concentrations so that

$$\frac{1}{s_{wa}} \simeq \frac{1}{s_2}(1 + gc) \tag{194}$$

If the slope of a plot of $1/s_{wa}$ vs c is taken at a very high concentration, one obtains g/s_2 as the slope and $1/s_2$ as the intercept of the tangent line at zero concentration. Clearly this method depends on where one draws the slope. There are ways to overcome this limitation; we will illustrate it with the second model (see Eq. 190).

Equation (190) suggests that a plot of $1/s_{wa}$ vs c behaves somewhat in a manner described by Fig. 20. The decrease in $1/s_{wa}$ is due to the self-association; the quantity gc increases linearly with c, so that the combination of the two factors causes a minimum in the plot of $1/s_{wa}$ vs c. This behavior is similar to that encountered with plots of M_1/M_{wa} vs c for nonideal self-associations. The actual shape of plots of $1/s_{wa}$ vs c depends

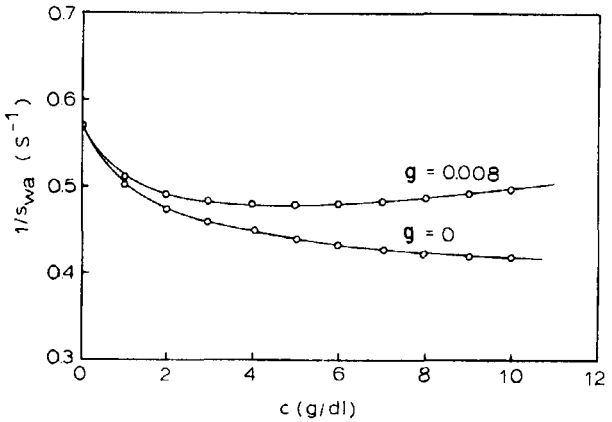

FIG. 20. Sedimentation coefficients of self-associating solutes. Here we used a simulated monomer–dimer association with $s_1 = 1.75s$, $s_2 = 2.85s$ and $K_2 = 0.35$ l/g. The lower curve shows a plot of $1/s_{wa}$ vs c for which there is no hydrodynamic concentration dependence ($g = 0$). Model II (Eq. 190) for describing s_{wa} was used here. The upper curve shows the effect of the hydrodynamic concentration dependence parameter ($g = 0.008$ l/g). Note the resemblance of these curves to plots of M_1/M_{wa} for self-associating solutes.

on the values of K_2, s_1, s_2, and g. The similarity of the plot of $1/s_{wa}$ vs c and M_1/M_{wa} vs c suggests that we try to develop equations that eliminate the gc term, so that the resulting equation only contains one or more unknowns (s_2, etc.). One way to eliminate g is to note that

$$\frac{1}{s_{wa}} - \frac{2}{c}\int_0^c \frac{dc}{s_{wa}} = \frac{1}{s_{wc}} - \frac{2}{c}\int_0^c \frac{dc}{s_{wc}} \tag{195}$$

For a monomer–dimer association, Eq. (195) becomes

$$\frac{1}{s_{wa}} - \frac{2}{c}\int_0^c \frac{dc}{s_{wa}} = \frac{1 + K_2c_1}{s_1 + K_2c_1s_2} + \frac{2}{c}\int_0^c \left(\frac{1 + K_2c_1}{s_1 + K_2c_1s_2}\right) dc \tag{196}$$

Since c_1, K_2, and s_1 are known, there is only one unknown, s_2, which is evaluated by successive approximations. The easiest way to evaluate $\int_0^c (dc/s_{wc})$ is to use a computer; for each choice of s_2, the integral has to be evaluated. Another way to estimate s_2 is to use the equation

$$\frac{1}{s_{wa}} - c\left[\frac{d(1/s_{wa})}{dc}\right] = \frac{1}{s_{wc}} - c\left[\frac{d(1/s_{wc})}{dc}\right] \tag{197}$$

This equation contains only one unknown, s_2, which can be evaluated by successive approximations. Once s_2 is known then it is possible to calculate g from the relation

$$\frac{1}{s_{wa}} - \frac{1}{s_{wc}} = gc \tag{198}$$

since a plot of $[(1/s_{wa}) - (1/s_{wc})]$ vs c has a slope of g. The analysis could also be done with the other model (Eq. 189) to describe s_{wa}, and the analysis can be extended to other self-associations, including a sequential, indefinite self-association. A test of these methods has been applied to the self-association of the γ-G globulin studied by Kakiuchi and Williams (*134*); the results are listed in Table 3. Note that g and g have different values. Also note that s_2 evaluated using either model, Eq. (189) or (190), to described s_{wa} agreed quite well with each other. The disagreement with the Kakiuchi and Williams method may reflect the fact that the value of s_2 depends on how and where one takes the tangent to the curve of $1/s_{wa}$ vs c.

It is also possible to evaluate s_{za}, the apparent z-average sedimentation coefficient (*42*, *135*), since with Model II (Eq. 190), s_{za} is given by

$$s_{za} = \frac{d(cs_{wa})}{dc} = s_{wa} + c\frac{d(s_{wa})}{dc} \tag{199}$$

TABLE 3
Estimation of s_2 from the Data of Kakiuchi and Williams (*134*)[a]

Model	s_2 (sec)	g (dl/g)	g (dl/g)
I (Eq. 189)	9.4[b]	0.32	—
I (Eq. 189)	10.3 ± 0.20[c]	0.35 ± 0.03	—
II (Eq. 190)	10.25 ± 0.20[d]	—	0.034 ± 0.0002

[a] $s_1 = 7.25$; $K_2 = 21.5$ dl/g.
[b] Values reported by Kakiuchi and Williams (*134*) using a method based on Eq. (194).
[c] Method based on Eq. (35) of Weirich, Adams, and Barlow (*42*); nine data points were used for estimating s_2.
[d] Method based on Eq. (197); see also Eq. (24) of Weirich, Adams, and Barlow. Twelve data points were used for the estimation of s_2.

One can also get s_{zc} or s_{za} with Model I. In fact, if one can measure any weight-average property, X_{wc}, of a self-associating solute, then it is possible to obtain the z-average property (*42*), X_{zc}, since

$$X_{zc} = \frac{d(cX_{wc})}{dc} = X_{wc} + c\frac{d(X_{wc})}{dc} \tag{200}$$

Here X_{wc} could be a weight-average partition coefficient, σ_{wc}, elution volume, $V_{e\,wc}$, or any weight or apparent weight-average property that can be measured. It is also possible to obtain a number-average property, X_{nc}, from a combination of equilibrium and transport methods (*42*). It should be evident that one can combine equations for X_{wc} or its apparent value, X_{wa}, in a manner similar to that done with s_{wc} or s_{wa} so that X_1, X_2, and other quantities, such as a concentration dependence parameter, can be evaluated. By combining equilibrium and transport techniques we can learn far more about the self-associating solute than we could learn from either technique alone. This is a very new development, and more work of this kind should appear in the future.

Acknowledgments

This work was supported by grants from the Robert A. Welch Foundation (A485) and from the National Science Foundation (GB 32242A1). Will E. Ferguson is a Robert A. Welch Foundation Postdoctoral Fellow.

REFERENCES

1. T. Svedberg and H. Rinde, *J. Amer. Chem. Soc.*, *46*, 2677 (1924).
2. J. D. Watson, *The Molecular Biology of the Gene*, 2nd ed., Benjamin, New York, 1970, p. 61.

3. T. Svedberg and K. O. Pedersen, *The Ultracentrifuge*, Clarendon, Oxford, 1940.
4. J. W. Williams, K. E. Van Holde, R. L. Baldwin, and H. Fujita, *Chem. Revs.*, *58*, 715 (1958).
5. H. Fujita, *Mathematical Theory of Sedimentation Analysis*, Academic, New York, 1960.
6. H. Rinde, Ph.D. Dissertation, University of Upsala, 1928.
7. J. S. Johnson, K. A. Kraus, and G. Scatchard, *J. Phys. Chem.*, *64*, 1867 (1960).
8. F. E. LaBar and R. L. Baldwin, *Ibid.*, *66*, 1952 (1962).
9. J. S. Johnson, K. A. Kraus, and G. Scatchard, *Ibid.*, *58*, 1034 (1954).
10. J. S. Johnson and K. A. Kraus, *Ibid.*, *63*, 440 (1959).
11. J. S. Johnson, K. A. Kraus, and R. W. Holmberg, *J. Amer. Chem. Soc.*, *78*, 26 (1956).
12. F. C. Hentz and J. S. Johnson, *Inorg. Chem.*, *5*, 1337 (1966).
13. J. S. Johnson, G. Scatchard, and K. A. Kraus, *J. Phys. Chem.*, *63*, 787 (1959).
14. J. Brandrup and E. H. Immergut, eds., *Polymer Handbook*, Wiley-Interscience, New York, 1966.
15. D. A. Albright and J. W. Williams, *J. Phys. Chem.*, *71*, 2780 (1967).
16. T. H. Donnelly, *Ibid.*, *70*, 1862 (1966).
17. T. H. Donnelly, *Ann. N. Y. Acad. Sci.*, *164*, 147 (1969).
18. Th. G. Scholte, *J. Polym. Sci.*, *A-2*, *6*, 111 (1968).
19. Th. G. Scholte, *Ann. N. Y. Acad. Sci.*, *164*, 156 (1969).
20. Th. G. Scholte, *Eur. Polym. J.*, *6*, 51 (1970).
21. S. W. Provencher, *J. Chem. Phys.*, *46*, 3229 (1967).
22. L.-O. Sundelöf, *Ark. Kemi*, *29*, 297 (1968).
23. M. Gehatia and D. R. Wiff, *Advan. Chem. Ser.*, *125*, 216 (1973).
24. E. T. Adams, Jr., P. J. Wan, D. A. Soucek, and G. H. Barlow, *Ibid.*, *125*, 235 (1973).
25. J. Vinograd and J. E. Hearst, *Fortschr. Chem. Org. Naturstoffe*, *20*, 372 (1962).
26. M. Meselson and F. W. Stahl, *Proc. Natl. Acad. Sci. U. S.*, *44*, 671 (1958).
27. S. Kaufman and A. J. Fryar, Paper presented at the 160th National Meeting of the American Chemical Society, Chicago, September 14–18, 1970. Abstract No. Coll 88.
28. J. J. Hermans, *Ann. N. Y. Acad. Sci.*, *164*, 122 (1969).
29. E. T. Adams, Jr., *Biochemistry*, *4*, 1646 (1965).
30. E. T. Adams, Jr., *Fractions*, No. 3, 1967.
31. D. A. Albright and J. W. Williams, *Biochemistry*, *7*, 67 (1968).
32. E. T. Adams, Jr. and M. S. Lewis, *Ibid.*, *7*, 1044 (1968).
33. K. E. Van Holde, G. P. Rossetti, and R. D. Dyson, *Ann. N. Y. Acad. Sci.*, *164*, 279 (1969).
34. P. W. Chun, S. J. Kim, J. D. Williams, W. T. Cope, L. H. Tang, and E. T. Adams, Jr., *Biopolymers*, *11*, 197 (1972).
35. L. H. Tang and E. T. Adams, Jr., *Arch. Biochem. Biophys.*, *157*, 520 (1973).
36. L. W. Nichol, J. L. Bethune, G. Kegeles, and E. L. Hess, in *The Proteins*, Vol. II, 2nd ed. (H. Neurath, ed.), Academic, New York, 1964, p. 305.
37. L. W. Nichol and D. J. Winzor, *Migration of Interacting Systems*, Clarendon, Oxford, 1972.
38. D. J. Winzor and H. A. Scheraga, *Biochemistry*, *2*, 1263 (1963); *J. Phys. Chem.*, *68*, 338 (1964).
39. G. K. Ackers, *Advan. Protein Chem.*, *24*, 343 (1970).
40. S. W. Henn and G. K. Ackers, *Biochemistry*, *8*, 3829 (1969).

41. P. W. Chun, S. J. Kim, C. A. Stanley, and G. K. Ackers, *Ibid.*, *8*, 1625 (1969).
42. C. A. Weirich, E. T. Adams, Jr., and G. H. Barlow, *Biophys. Chem.*, *1*, 35 (1973).
43. P. J. Wan, Ph. D. Dissertation, Texas A & M Univ. College Station, Texas, December 1973.
44. P. J. Wan and E. T. Adams, Jr., *Polym. Preprints*, *15*, 509 (1974).
45. M. Gehatia and D. R. Wiff, *J. Polym. Sci.*, *A-2*, *8*, 2039 (1970).
46. M. Gehatia, *Polym. Preprints*, *12*, 875 (1971).
47. D. R. Wiff and M. Gehatia, *J. Macromol. Sci.—Phys.*, *B6*, 287 (1972).
48. M. Gehatia and D. R. Wiff, *Eur. Polym. J.*, *8*, 585 (1972).
49. M. Gehatia and D. R. Wiff, *J. Chem. Phys.*, *57*, 1070 (1972).
50. E. T. Adams, Jr., in *Characterization of Macromolecular Structure*, Publication 1573, National Academy of Sciences, Washington, D.C., 1968, p. 106.
51. W. D. Lansing and E. O. Kraemer, *J. Amer. Chem. Soc.*, *57*, 1369 (1935).
52. J. W. Williams, *Ultracentrifugation of Macromolecules*, Academic, New York, 1972.
53. R. L. Baldwin and K. E. Van Holde, *Fortschr. Hochpolym.-Forsch.*, *1*, 451 (1960).
54. H. W. McCormick, in *Polymer Fractionation* (M. J. R. Cantow, ed.), Academic, New York, 1967, p. 251.
55. M. Wales and S. J. Rehfeld, *J. Polym. Sci.*, *62*, 179 (1962).
56. J.-P. Merle and A. Sarko, *Macromolecules*, *5*, 132 (1972).
57. T. Bluhm and A. Sarko, *Ibid.*, *6*, 578 (1973).
58. D. J. DeRosier, P. Munk, and D. J. Cox, *Anal. Biochem.*, *50*, 139 (1972).
59. L. J. Gosting, *J. Amer. Chem. Soc.*, *74*, 1458 (1952).
60. J. W. Williams, W. M. Saunders, and J. S. Cicirelli, *J. Phys. Chem.*, *58*, 774 (1954).
61. J. W. Williams and W. M. Saunders, *Ibid.*, *58*, 854 (1954).
62. J. C. Moore, in *Characterization of Macromolecular Structure*, Publication 1573, National Academy of Sciences, Washington, D.C., 1968, p. 273.
63. M. Ezrin (ed.), *Polymer Molecular Weight Methods*, American Chemical Society Advances in Chemistry Series No. 125, 1973.
64. K. A. Granath, *J. Colloid Sci.*, *13*, 308 (1958).
65. K. A. Granath, *Makromol. Chem.*, *28*, 1 (1958).
66. J. W. A. Averink, H. Reerink, J. Boerma, and W. J. M. Jaspers, *J. Colloid Interface Sci.*, *21*, 66 (1966).
67. H. J. Cantow, *Makromol. Chem.*, *70*, 130 (1964).
68. O. Bryngdahl and S. Ljunggren, *J. Phys. Chem.*, *64*, 1264 (1960).
69. P. J. Debye, *J. Phys. Colloid Chem.*, *51*, 18 (1947); *Ann. N. Y. Acad. Sci.*, *51*, 575 (1949); *J. Phys. Colloid Chem.*, *53*, 1 (1949).
70. E. W. Anacker, R. M. Rush, and J. S. Johnson, *J. Phys. Chem.*, *68*, 81 (1964).
71. S. Ikeda and K. Kakiuchi, *J. Colloid Interface Sci.*, *23*, 134 (1967).
72. H.-G. Elias, *J. Macromol. Sci.—Chem.*, *A7*, 601 (1973).
73. K. E. Van Holde and G. P. Rossetti, *Biochemistry*, *6*, 2189 (1967).
74. T. N. Solie and J. A. Schellman, *J. Mol. Biol.*, *33*, 61 (1968).
75. P. O. P. T'so, *Ann. N. Y. Acad. Sci.*, *153*, 785 (1969).
76. H.-G. Elias and R. Bareiss, *Chimia*, *21*, 53 (1967).
77. A. Tiselius, *Z. Phys. Chem.*, *124*, 449 (1926).
78. R. F. Steiner, *Arch. Biochem. Biophys.*, *39*, 333 (1952); *44*, 120 (1953).
79. R. F. Steiner, *Ibid.*, *49*, 400 (1954).
80. M. S. N. Rao and G. Kegeles, *J. Amer. Chem. Soc.*, *80*, 5724 (1958).

81. E. T. Adams, Jr., and H. Fujita, in *Ultracentrifugal Analysis in Theory and Experiment* (J. W. Williams, ed.), Academic, New York, 1966, p. 119.
82. E. T. Adams, Jr., and J. W. Williams, *J. Amer. Chem. Soc.*, *86*, 3454 (1964).
83. M. Derechin, *Biochemistry*, *7*, 3253 (1968); *8*, 921, 927 (1969); *11*, 1120, 4153 (1972).
84. M. Derechin, Y. M. Rustrum, and E. A. Barnard, *Ibid.*, *11*, 1793 (1972).
85. K. Šolc and H.-G. Elias, *J. Polym. Sci., Polym. Phys. Ed.*, *11*, 137 (1973).
86. A. Vrij and J. Th. G. Overbeek, *J. Colloid. Sci.*, *17*, 570 (1962).
87. E. F. Casassa and H. Eisenberg, *Advan. Protein Chem.*, *19*, 287 (1964).
88. H. Edelhoch, E. Katchalski, R. H. Maybury, W. L. Hughes, Jr., and J. T. Edsall, *J. Amer. Chem. Soc.*, *75*, 5058 (1953).
89. E. Braswell, *J. Phys. Chem.*, *78*, 2477 (1968).
90. E. T. Adams, Jr., *Biochemistry*, *4*, 1655 (1965).
91. J. Visser, R. C. Deonier, E. T. Adams, Jr., and J. W. Williams, *Ibid.*, *11*, 2634 (1972).
92. P. J. Flory, *Principles of Polymer Chemistry*, Cornell Univ. Press, Ithaca, New York, 1953. Chap. 8.
93. L.-H. Tang, Ph.D. Dissertation, Illinois Institute of Technology, Chicago, December 1971.
94. F. S. Acton, *Numerical Methods That Work*, Harper and Row, New York, 1970.
95. L.-H. Tang, B. M. Escott, and E. T. Adams, Jr., Unpublished Material.
96. P. W. Chun, *Biophys. J.*, *10*, 563, 577 (1970).
97. A. H. Pekar and B. H. Frank, *Biochemistry*, *11*, 4013 (1972).
98. C. Tanford, *Physical Chemistry of Macromolecules*, Wiley, New York, 1961, p. 7.
99. W. E. Ferguson, C. M. Smith, E. T. Adams, Jr., and G. H. Barlow, *Biophys. Chem.*, *1*, 325 (1974).
100. W. E. Ferguson, B. M. Escott, J. L. Sarquis, P. J. Wan, E. T. Adams, Jr., and G. H. Barlow, Unpublished Material.
101. D. C. Teller, *Biochemistry*, *9*, 4201 (1970).
102. K. Kakiuchi, *J. Phys. Chem.*, *69*, 1829 (1965).
103. S. N. Timasheff and R. Townend, *J. Amer. Chem. Soc.*, *83*, 470 (1961).
104. J. L. Sarquis and E. T. Adams, Jr., *Arch. Biochem. Biophys.*, *163*, 442 (1974).
105. H. A. McKenzie, *Milk Proteins*, Vol. 2, Academic, New York, 1971, Chap. 14.
106. R. Townend and S. N. Timasheff, *J. Amer. Chem. Soc.*, *82*, 3168 (1960); S. N. Timasheff and R. Townend, *Ibid.*, *83*, 464 (1961); T. F. Kumosinski and S. N. Timasheff, *Ibid.*, *88*, 5635 (1966).
107. H. A. McKenzie, *Milk Proteins*, Vol. 1, Academic, New York, 1970, p. 215.
108. D. G. Schmidt, Ph.D. Dissertation, University of Utrecht, Utrecht, The Netherlands, 1969.
109. G. W. Richter and G. F. Walker, *Biochemistry*, *6*, 2871 (1967).
110. D. K. Hancock and J. W. Williams, *Ibid.*, *8*, 2598 (1969).
111. J. W. Williams, *Ultracentrifugation of Macromolecules*, Academic, New York, 1972.
112. H. Eisenberg and G. Tompkins, *J. Mol. Biol.*, *31*, 37 (1968).
113. R. Josephs, H. Eisenberg, and E. Reisler, *in Protein-Protein Interactions* (R. Jahnicke and E. Helmreich, eds.), Springer, New York, 1972, p. 57.
114. P. W. Chun, S. J. Kim, C. A. Stanley, and G. K. Ackers, *Biochemistry*, *8*, 1625 (1969).

115. S. N. Timasheff, in *Proteides of the Biological Fluids* (Proceedings of the 20th Colloquium Brugge, 1972), (H. Peeters ed.), Pergamon, Oxford, 1973, p. 511.
116. J. B. Harry and R. F. Steiner, *Biochemistry*, *8*, 5060 (1969).
117. P. O. P. T'so, I. S. Melvin, and A. C. Olson, *J. Amer. Chem. Soc.*, *85*, 1289 (1963).
118. G. A. Gilbert, *Discussions Faraday Soc.*, *20*, 68 (1955); *Proc. Roy. Soc. A*, *250*, 377 (1959).
119. G. A. Gilbert and R. C. Ll. Jenkins, *Ibid.*, *A*, *253*, 420 (1959).
120. L. M. Gilbert and G. A. Gilbert, *Nature*, *194*, 1173 (1962).
121. G. A. Gilbert, *Proc. Roy. Soc.*, *A*, *276*, 354 (1963).
122. D. J. Cox, *Arch. Biochem. Biophys.*, *142*, 514 (1971).
123. D. J. Cox, *Ibid.*, *146*, 181 (1971).
124. W. B. Goad and J. R. Cann, *Ann. N. Y. Acad. Sci.*, *164*, 172 (1969).
125. J. R. Cann, *Interacting Macromolecules*, Academic, New York, 1970.
126. H. Fujita, *Mathematical Theory of Sedimentation Analysis*, Academic, New York, 1960, pp. 209–215.
127. L. W. Nichol and H. A. McKenzie, in *Milk Proteins*, Vol. 1 (H. A. McKenzie, ed.), Academic, New York, 1970, pp. 280–288.
128. L. W. Nichol, J. L. Bethune, G. Kegeles, and E. L. Hess, in *The Proteins*, Vol. 2, 2nd ed. (H. Neurath, ed.), Academic, New York, 1964, p. 305.
129. K. Granath and P. Flodin, *Makromol. Chem.*, *48*, 160 (1961).
130. E. E. Brumbaugh and G. K. Ackers, *J. Biol. Chem.*, *243*, 6315 (1968).
131. G. K. Ackers, *Advan. Protein Chem.*, *24*, 343 (1970).
132. S. W. Henn and G. K. Ackers, *Biochemistry*, *8*, 3829 (1969).
133. W. Godschalk, *Ibid.*, *10*, 3284 (1971).
134. K. Kakiuchi and J. W. Williams, *J. Biol. Chem.*, *241*, 2781 (1966).
135. G. Kegeles, *Proc. Nat. Acad. Sci. U.S.*, *69*, 2577 (1972).

Received by editor July 27, 1974

SYMPOSIUM TO BE CONTINUED